

Power Plant Design using Allam Cycle CCS

A Technical Report submitted to the Department of Chemical Engineering

Presented to the Faculty of the School of Engineering and Applied Science

University of Virginia • Charlottesville, Virginia

In Partial Fulfillment of the Requirements for the Degree

Bachelor of Science, School of Engineering

Spring, 2021.

Technical Project Team Members

Michael Beekwilder

Benjamin Johnson

Conor Moran

Jay Perry

Alexander Sims

On my honor as a University Student, I have neither given nor received unauthorized aid on this assignment as defined by the Honor Guidelines for Thesis-Related Assignments

Eric W. Anderson, Lecturer in Chemical Engineering, Department of Chemical Engineering

Abstract

This process produces commercial power capable of outputting 618 MWe at peak operating capacity. The plant is also capable of capturing all CO₂ emissions and sequestering or selling it for enhanced oil recovery. The plant produces its electricity by taking in 1.25 kmol/s of natural gas and 2.5 kmol/s of nominally pure O₂, which is obtained from an on site air separation unit. In contrast, the plant outputs 2.48 kmol/s of waste water and 1.29 kmol/s of vapor exhaust. The vapor exhaust is over 90% molar purity CO₂ with the rest being predominantly CO and trace amounts of water.

The power plant's initial capital investment will be \$57.9 million USD. The operating expenses are expected to predominantly come from raw materials. The oxygen is estimated to cost \$0.07 USD per kg. The natural gas contract is expected to result in a cost of \$0.009 USD per kilogram. While the oxygen will be nominally pure, the natural gas will contain a mixture of hydrocarbons. There are only expected to be very trace amounts of Nitrogen and other pollutants which allows for zero costs in waste removal. The expected yearly revenue from the plant will come from electricity and CO₂ sales. The electricity is expected to sell at \$ 46.54 USD per megawatt hour while the CO₂ is expected to sell for \$40.00 USD per metric ton. In total, the annual revenue is expected to be \$184.94 million USD per year while the annual costs of manufacturing are expected to be \$189.06 million USD per year without depreciation. Because the standard cost of manufacturing is greater than the expected process revenues, this plant would not yield an annual return and therefore could not possibly provide an acceptable ROI for investment. Lowering the purchasing cost of oxygen or increasing the selling price of electricity by marginal amounts can make the plant profitable. Additionally, implementation of an on-site air separation unit (ASU) would reduce costs and increase revenue to make the plant feasible.

Table of Contents

1. Introduction	4
1.1 Climate Background	4
1.2 CCS Technology	5
1.3 Allam Cycle CCS	6
2. Previous Work	7
3. Design Discussion	8
3.1 Fundamental Principles and Design Basis	8
3.1.1 System Kinetics and Thermodynamics	8
3.1.2 Allam Cycle Process Description	10
3.1.3 Scale	12
3.2 Technical Matters of Importance	13
3.2.1 Property Methods and Setup in Aspen Plus	13
3.2.2 Inputs and Outputs	13
3.2.3 Unit Operations	18
3.2.4 Plant Location Choice and Implications	26
3.2.5 Electricity Utility	28
3.2.6 Cooling Water Utility	29
3.2.7 Difficulties in Design	30
4. Final Recommended Design	34
4.1 Process Flow Diagram	34
4.2 Equipment Tables and specifications	35
4.3 Material and Energy Balances	37
4.4 Process Economics	39
4.4.1 Capital Costs	39
4.4.2 Operational Costs	41
4.4.3 Revenues	44
4.4.4 ROI	45
5. Safety, Health, and Environmental	47
5.1 Material Compatibility	47
5.2 Credible Events	48
5.2.1 Loss of Primary Containment	48
5.2.2 Temperature Fluctuations	49
5.2.3 Pressure Fluctuations	50
5.2.4 Process Flow Fluctuations	51
5.2.5 Explosions and Flammability	51

5.3 Modeling of Release	52
5.4 Waste Stream Disposal	58
5.5 Toxicity	60
6. Conclusions and Recommendations	63
6.1 Financial Considerations	63
6.2 Recommendations and Future Work	64
7. Acknowledgements	67
8. Table of Nomenclature	68
9. References	72
10. Appendix	77
10.1 Equations	77
10.2 Sample Calculations	80
10.3 Computer Software	83
10.3.1 AspenPlus v11	83
10.3.2 CHEMKED II	83
10.3.3 Microsoft Excel	83
10.3.4 ALOHA/CAMEO/MARPLOT	83
10.3.5 CRW	84
10.4 Primary Reactions	84
10.5 Equipment Capital Costs	85
10.6 Other Data	86

1. Introduction

1.1 Climate Background

As energy demands across the globe rise due to rising populations and standards of living, the consumption of fossil fuels will also rise. There is simply not enough renewable

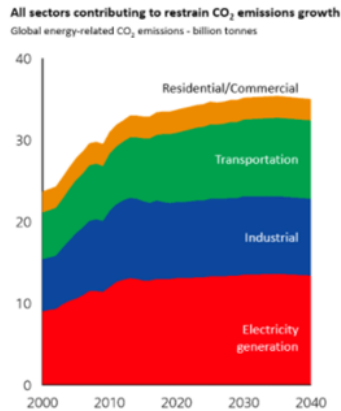


Figure 1-1: Timeline of Global CO₂ Emissions broken down by sector

energy available to support current energy needs, which means that fossil fuels will be a staple of energy production for most of the 21st century (Crane, 2020). ExxonMobil's 20 year energy outlook predicts that in 2040, 76% of the world's energy will still be produced by fossil fuels

(Crane, 2020). The Intergovernmental Panel on Climate Change (IPCC) report to

the UN found that global temperatures have already risen by 1.0°C from pre-industrial times and are likely to be 1.5°C higher than pre-industrial times by 2030. With the Paris agreement setting 2.0°C as the upper limit for anthropogenic global warming, there needs to be rapid changes to emissions to meet this goal. It is estimated that carbon dioxide (CO₂) is currently emitted into the atmosphere at a rate of 36.6 gigatons per year (Figure 1-1), and to achieve a 2°C pathway, no more than 565 gigatons more of CO₂ may be released to the atmosphere over the coming years. Furthermore, Figure 1-1 shows that the electricity generation sector produces approximately 33% of global CO₂ emissions. The combination of rising emissions and an already large global emissions output has set the world off course from the 2°C pathway: projections show that this 2°C increase will likely be surpassed by 2035. According to the IPCC report, "Reaching and

sustaining net zero global anthropogenic CO₂ emissions and declining net non-CO₂ radiative forcing would halt anthropogenic global warming on multi-decadal timescales”.

1.2 CCS Technology

To achieve the reduced emissions necessary to reverse anthropogenic global warming, a technological shift has to occur away from fossil fuel based power generation, and towards Renewable Energy Technology (RET). The shift from traditional fossil fuel technology to RET however is a big one and cannot happen overnight. To assist in this necessary transition is the concept of “bridge technologies,” which is technology employed that reduces the negative impact of incumbent power generation methods while the infrastructure for RET is being developed on a large scale. Carbon Capture and Sequestration (CCS) is one of these aforementioned bridge technologies. The concept of capturing carbon and storing it before it can be released into the atmosphere was first proposed sometime in the 1970s (IEAGHG, 2012). The process captures CO₂ via three different methods, pre-combustion, post-combustion, and oxyfuel combustion. Pre-combustion capture refines the fuel of carbon elements before it is combusted, post-combustion separates out the CO₂ from the flue gas exhaust and Oxy-fuel combusts the fuel with pure oxygen gas (O₂) with a gas shift reaction to form easily separable water (H₂O) and CO₂. This practice was first utilized in processing facilities that separated excess CO₂ from natural gas and injected it into oil fields in a process called enhanced oil recovery (EOR). All three of these methods effectively capture the CO₂ from the process, but have heavy energy penalties, ranging from 5-40%. This major drawback makes CCS economically unattractive, which has limited CCS implementation - CCS may only see widespread use by severely reducing these associated energy penalties.

1.3 Allam Cycle CCS

The Allam cycle, proposed in 2013 by Rodney Allam, offers a promising potential gain in economic viability for CCS (Allam et al., 2013). The process adapts well to the current U.S. energy industry through compatibility with the abundance of U.S. natural gas and coal reserves and the removal of emissions concerns. This cycle provides an emission-free complement to renewable energies that can ensure energy demand is met under conditions where renewables cannot achieve their maximum outputs (lack of sun or wind). The Allam cycle is able to achieve a lower energy penalty as well as zero atmospheric carbon emissions by using supercritical CO₂ as a working fluid to create a modified version of the Brayton cycle. It begins with a high pressure oxy-fuel combustor that combusts natural gas largely, composed of methane, with pure O₂ and recycled CO₂ streams. The byproducts of the combustion are only CO₂ and water. The high-pressure outlet stream is then fed to a turbine that will generate power. The exhaust of this combustion gets separated, and then used to create a partially closed loop using the majority of the CO₂ for working fluid, and exporting all water. This novel power cycle fills the energy sector's vacant niche as a technology that simultaneously takes advantage of the massive US natural gas reserves while minimizing carbon emissions.

2. Previous Work

There are two main existing literature pieces that focus on the design and implementation of the Allam cycle for power generation. Both documents were written by Rodney Allam and discuss the development and scale up of power plants that utilize his cycle. The first document, written in 2013 introduces the Allam cycle as a modified Brayton cycle that uses supercritical CO₂ as the working fluid (R. Allam et al., 2013). Allam outlines his cycle for both coal and gas burning power plants. Included in this document are some motivations for why CCS is a valuable technology to include in power generation facilities, as well as a description of designs used for specific unit operations that make the plant run. The core of the paper focuses on developing a 50 MWe pilot plant in Texas to prove that the concept works.

The second document, written in 2017, focuses on the development of a 300 MWe scale up plant. The paper updates the PFD given for the 50 MW demo plant and gives more detailed descriptions of the thermodynamics behind the cycle. In this paper, Aspen Plus is specifically cited as being the main modeling software used by Allam. Also included in the 2017 paper are more in depth descriptions of the designs of certain unit operations. In particular, special designs of the main turbine and the recuperator are given (R. Allam et al., 2017). The rest of the paper focuses on updates to economic promises and opportunities that scaling up the Allam cycle would present.

In both of these papers, the main focus is providing proof of concept and describing the necessary technology in detail. Allam successfully demonstrated that the 50 MWe is feasible and lays out how the 300 MWe will not only match efficiencies of other power cycles, but match the economic viability of traditional plants. The aim of this study is to fill a gap in the existing literature by designing a fully commercial Allam cycle power plant.

3. Design Discussion

3.1 Fundamental Principles and Design Basis

3.1.1 System Kinetics and Thermodynamics

The primary reaction in this cycle is the combustion of methane given by Reaction 1 in appendix 10.3.5. Despite the seeming simplicity of the overall reaction, it does not break into a small number of elementary steps. Depending on the study, the reaction mechanism can take anywhere from 325 to over 1000 elementary reactions to accurately describe. Because of the complexity involved in describing the reaction mechanisms, the kinetics of the methane combustion are very complicated to do by hand using basic kinetic modeling methods. In contrast, the thermodynamics of methane combustion are well understood and can easily be modeled by equations of state. The two best equations of state to model combustion are RK-Soave and Peng-Robinson.

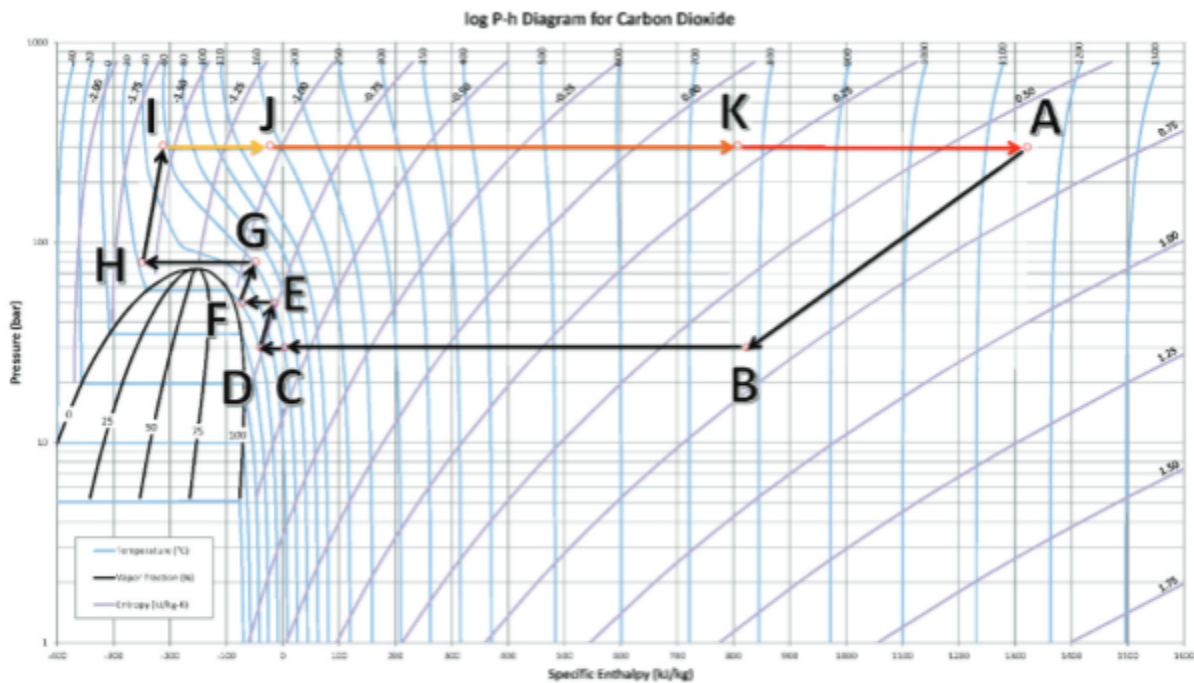


Figure 3-1: Pressure -Enthalpy Chart for CO₂ During Allam Cycle (R. Allam et al., 2017)

In this study, methane combustion drives the Allam cycle, which is a modification of the Brayton cycle. Because CO₂ is the working fluid, it is worth discussing the enthalpy and pressure changes throughout the cycle to get a better picture of the thermodynamics. As seen in Figure 3-1, the working fluid undergoes similar pressure and enthalpy changes expected in conventional power cycles. Point A represents the inlet to the turbine, while point B represents the outlet. The pressure and enthalpy drop here is due to the mechanical work the exhaust CO₂ stream is doing to generate electricity. From point B to point C the exhaust stream is transferring heat to recycle streams before undergoing compression. Points C to D represent further cooling done to remove water generated from combustion. Points D-G represent multistage compression with intercooling at the low pressure end of the cycle. After compression, the CO₂ is cooled to ambient temperatures which is denoted in points G-H. It should be noted that point G is picked such that its pressure is just above the critical pressure of CO₂. Cooling to ambient temperatures results in a significant density increase that allows for easier compression back to high pressures from points H to I. Waste heat from compressors, or a nearby ASU is used to provide heat from points I to J. The heat given off by the low pressure exhaust in the recuperator is absorbed giving the increase of enthalpy seen in points J to K, while the heat of combustion gives the remaining heat to get from point K to A (R. Allam et al., 2017).

feed. In the context of this project, the ASU will be black boxed, but is a LOX style cryogenic air separator (R. Allam et al., 2017). Upon expansion through the turbine, the exhaust stream consisting of CO₂ and water experiences a pressure and temperature reduction. This exhaust stream also flows through the recuperating heat exchanger in order to transfer heat to the CO₂ recycle stream before moving to a separation unit (R. Allam et al., 2017).

After the exhaust stream from the turbine passes through the recuperator, the stream is further cooled. The stream is then passed through a flash separator that condenses out the water produced from the combustion in the turbine. The water has a nominally high purity and can be disposed of without further processing. The remaining gaseous CO₂ stream, now slightly cooler than before passing through the water separator, passes through a CO₂ compressor. Compressing the stream increases the temperature, and so it is sent through another heat exchanger to bring the temperature back down to post water separation temperatures.

Before the CO₂ stream is cooled again, a portion of it is taken off as a product stream. This is a very high purity CO₂ stream, which is pumped to a high pressure CO₂ pipeline where it can be sold to an enhanced oil recovery process so that they sequester it through their process. Overall, about 5% of the mass of the recycle stream is taken out as a product. After cooling, the recycle stream is split into two separate streams. The first of these new streams is sent to the recycle compressor while the other stream is mixed with pure oxygen from the ASU and then fed to an oxidant pump. Both of these streams are then fed to the recuperator and are used to help cool the product exhaust stream (R. Allam et al., 2017). The reason why the streams are split goes back to the specially designed combustion chamber by Toshiba. Natural gas and the oxygen containing stream are passed directly through the flame in the combustion chamber while the non-oxygenated CO₂ stream does not pass directly through the flame. Instead, it is used as a

quenching stream and is passed through the combustion chamber to act as a heat sink and reduce the overall temperature of the exit stream. A portion of this stream is also passed through concurrent shells in the turbine to help cool it as well.

3.1.3 Scale

With rising living standards and exponential populations growth, global electricity requirements are expected to grow significantly during the foreseeable future. In fact, the U.S. Energy Information Administration (EIA) predicts that electricity consumption in all U.S. energy sectors will increase by 2.1% in 2021 (*Short-Term Energy Outlook - U.S. Energy Information Administration (EIA)*, n.d.). It is imperative that large scale power plants projects continue to be commissioned to meet this growth in electricity demand, ideally utilizing new high efficiency technologies and emissions control systems.

For CCS technologies to permeate into the energy sector, they must have proven feasibility at large scales. A 50 MW Allam cycle pilot plant was built in 2018 in La Porte, TX by Net Power and proved that the Allam cycle can produce electricity at high efficiencies comparable to Natural Gas Combined Cycle (NGCC) power plants (R. Allam et al., 2017). Net Power has also extensively designed a moderately sized 300 MWe commercial Allam cycle power plant that was planned for 2022 in the hopes of further proving the viability of the technology (Patel, 2019). Scaling CCS technologies rapidly is challenging, and unforeseen issues at too large of scales could threaten the perceived feasibility of the technology, leading to abandonment. According to the EIA, the average NGCC power block has a capacity of 820 MWe in 2017 (*Power Blocks in Natural Gas-Fired Combined-Cycle Plants Are Getting Bigger - Today in Energy - U.S. Energy Information Administration (EIA)*, n.d.). Although the overarching goal of this project is to design a large scale commercial Allam cycle power plant that is

environmentally superior to today's average NGCC plant, a balance had to be struck between conservative scale-up and proof of concept at large scales. Consequently, this project aimed to design a 600 MWe Allam cycle power plant as the next step in proving the viability of Allam's technology. This estimate comes from comparison to the existing net 300 MWe power plant, which we assume will operate at the same efficiency as the proposed plant (Goff, 2019).

3.2 Technical Matters of Importance

3.2.1 *Property Methods and Setup in Aspen Plus*

This Allam Cycle design was modeled in Aspen Plus using the Peng Robinson equation of state. Modeling this process in Aspen Plus allowed for total process simulation to obtain stream results as well as unit operation data. Peng-Robinson was chosen as the best equation of state to match the operating conditions of this cycle as it is well suited for modeling hydrocarbons and non-polar substances. Furthermore, Peng Robinson EOS is also a suitable property modeling method at high temperature and pressure states such as in hydrocarbon processing, or supercritical scenarios. This process as designed handles hydrocarbon combustion at temperatures and pressures up to 1200 °C and 300 bar, and recycles CO₂ at supercritical conditions. Based on the operation parameters and general lack of polar components in the process, Peng Robinson was able to be chosen as the preferred EOS for modeling.

3.2.2 *Inputs and Outputs*

The primary input reactants for the Allam cycle are O₂ and methane (CH₄), with a starting amount of CO₂ for the working fluid. During start-up, CO₂ is necessary as a starting material because it operates as the working fluid to carry heat through the system. The existing Allam cycle plant incorporates CO₂ into the loop at 882.8 kg/s with conditions of 16°C and 100 bar (R.

Allam et al., 2017; R. Allam et al., 2013). Once the process reaches steady state, CO₂ is produced as a product and will no longer need to be added into the system.

In assessing the input methane source, this power generation facility follows suit with other natural gas power facilities that use pipelines to pump in natural gas fuel as a vapor. The natural gas brought into the facility is at 40 bar and 25°C (R. Allam et al., 2013). The input pipeline natural gas is 80-99% methane, with the remaining percent made of small quantities of ethane, nitrogen, and CO₂. These impurities are low enough such that there is no concern over NO_x and other emissions (R. Allam et al., 2013).

The input oxygen source was originally going to be received from an on-site air separation unit (ASU), but the economics of this choice were not favorable and was abandoned. Pure oxygen gas is pumped straight into the plant from an off-site pipeline in a gaseous state and at a pressure of 100 bar. The Allam Cycle produces high-quality, high-value products in electricity, CO₂ and water. Electricity and carbon dioxide are the main focus of what happens to the products. This is expected due to assumed complete combustion being accomplished in the combustor. The predominant product, the electricity generated, will be sold for revenue to municipalities or other professional industries.

The water product has many opportunities. While selling to municipalities would be an attractive solution, most cities and their populations are not keen to the idea that their drinking water comes from a fossil fuel power plant (Blau, 2020); this is seen in agriculture as well. There are opportunities in fields like fracking or nuclear power that would likely be more open to purchasing the separated water (Goodyear, 2013). However, the most likely scenario would be re-introduction to the environment via evaporation ponds or discharge after clearance from

hazardous material authorities. This course of action was decided upon and is explored in Section 5.4 in depth.

This Allam cycle power plant is also capable of producing carbon dioxide, which is separated and removed from the system for repurposing in the EOR industry. This method extracts value out of the CO₂ produced from this process, and actively works to sequester carbon with low chances of leakage to the atmosphere, an important characteristic of the project as a whole. To meet EOR specifications, the output stream must be at least 90wt% CO₂ and must contain less than 5wt% carbon monoxide (CO) (Verma, 2015).

A possible side-product to be wary of within this process is CO that does not eventually shift to CO₂. While it was assumed that no CO would be produced through combustion, it was important to plan for its presence in reality. Should CO be present in the water output stream, it would need to be monitored and possibly separated or transformed before the product leaves the facility.

The Aspen model eventually reconfigured the input stream conditions and flow rates to best optimize the project as seen in Table 4-3 through Table 4-6. The pipeline fuel is piped in with a flow rate of 21.05 kg/s at the previously mentioned 40 bar and 25 °C with a 95% majority CH₄ molar composition in the vapor phase, supplemented by trace amounts of nitrogen gas (N₂), CO₂ and ethane (C₂H₆). The O₂ is piped in with a flow rate of 80 kg/s at 100 bar and 16 °C as a pure O₂ vapor. The process then outputs a water stream and a mixed product stream with mainly CO₂. The water stream exits the flash drum separator at 26.9 bar and 17 °C at a rate of 44.65 kg/s. This stream is 99.97 wt% H₂O with a trace amount of CO₂ and negligible amounts of CO, H₂, N₂, and O₂. The final product stream then leaves the process after being separated from the

recycle stream in a liquid state at a rate of 56.39 kg/s at a pressure of 100 bar and a temperature of 23 °C. This stream is composed of CO₂ as 98% mole fraction and 2% mole fraction of N₂ gas.

Fuel Requirement Estimation

The approach used for the preliminary calculation of fuel input required for this 600 MWe Allam cycle plant is based on the combination of an energy balance and multiple reactive material balances across the entire system boundaries. This includes all elements of the power cycle. To develop the baseline for these balances, it was assumed that the process is running at steady-state conditions and that the inlet and outlet streams have negligible changes in potential and kinetic energy as only changes in enthalpy are relevant. The general form of this overall energy balance is described by Equation 3-14.

Further assumptions were necessary to extract useful quantities from these balances. It was assumed that the effects of partial combustion are negligible, and that complete combustion dominates the process (no CO produced). Additionally, it was assumed that complete conversion of the limiting reactant (O₂) is achieved in the process, necessitating that the outlet CO₂ stream contain no oxygen. The effects of trace elements in the inlet air stream (Ar, CO₂, CO, and water vapor) were also ignored, which helped simplify the material and energy balances on the system. The last important assumption made for these preliminary calculations is that the natural gas fuel input can be approximated as pure methane at the average of natural gas pipeline pressures (40 bar) (R. Allam et al., 2013).

To assist in solving the overall energy balance to determine the required fuel input to achieve 600 MWe net of power, flow rates of all streams were expressed in terms of the methane fuel input, which was accomplished using reactive mole balances under the assumption of 100% conversion of O₂ and complete combustion. These relationships can be seen below as Equations

3-15 to 3-19. By substituting these relationships into the overall energy balance, the balance was rewritten in the form of Equation 3-20. Using a reference state of 25°C and 1 atm, the enthalpy of every inlet and outlet stream was determined according to that stream’s temperature and pressure – these values can be seen in Table 3-1. Using these enthalpies, the designed net power output (600 MWe), the assumed overall efficiency of the process (0.589), and the initial proposed fuel excess ($\alpha = 0.05$), the initial required molar and mass flow rate of methane feed was determined. Using the relationships in Equations 3-15 through 3-19, the molar and mass flow rates of all other streams were determined. The stream flow rate results can be seen in Table 3-1 and serve as a base estimation of the scale of this project. It should be noted that the Air Feed and N₂ Outlet streams were not part of the final design proposal after the ASU was black-boxed.

Table 3-1: Stream Characteristics under Initial Fuel Estimation

Stream	Temperature (°C)	Pressure (bar)	Enthalpy (kJ/mol)	Molar Flow Rate (kmol/s)	Mass Flow Rate (kg/s)
CH ₄ Feed	25	40.0	-75.07	1.11	17.78
Air Feed	25	1.01	-5.01	10.05	291.29
O ₂ Feed	25	1.01	--	2.11	67.53
CH ₄ Outlet	23	100	-75.14	0.05	0.85
CO ₂ Outlet	23	100	-393.67	1.06	46.46
N ₂ Outlet	-196	1.01	-6.44	7.94	222.57
H ₂ O Outlet	17	29	-242.36	2.11	38.03

* Enthalpies determined from a reference state of 1 atm and 25°C. Enthalpies collected from (*Engineering Software -- Physical Properties Calculator ...*, n.d.)

In addition to the energy balance, a proportion-based scale up of thermal input of the 303 MWe plant was used to check the magnitude of the calculated fuel input – this proportion can be seen in Equation 3-21 (Goff, 2019). While on the same order of magnitude, there was a notable discrepancy between the methane flow rates determined from the energy balance (17.78 kg/s) and the proportion (15.45 kg/s). While the exact cause for this discrepancy is unknown, it is likely a direct result of the multitude of assumptions made in order to utilize an overall energy

balance. Another reason for this discrepancy may be that a proportional scale-up is not an accurate representation of how scale affects fuel requirements, and that a non 1:1 relationship may exist. Nevertheless, the fairly close agreement in magnitude between these values allows for a trustworthy first estimate of the fuel requirement necessary to produce 600 MWe from a large-scale Allam power cycle. This initial estimation of the fuel input was adapted several times throughout the duration of the project to be optimized. These adaptations are detailed in Section 3.2.7.

3.2.3 Unit Operations

Combustor

According to Allam, the combustor employed for the pilot plant uses a complex input arrangement where natural gas and oxidant are fed simultaneously with an additional CO₂ quench stream fed to the combustor further down the tube length. Modeling this arrangement entirely with a single unit is difficult in Aspen Plus; therefore, two reactor blocks and a turbine were chosen to approximate the arrangement. The first block was to be designed as an adiabatic RGIBBS reactor that was fed natural gas and a mixed oxidant-CO₂ stream. The resulting high temperature exhaust was fed to the second adiabatic RGIBBS reactor along with the CO₂ quench stream. The exhaust out of the first combustor allowed for an estimation of what the flame temperature would be in the real combustion chamber, which Aspen calculated to be 1827.8 °C.

While it was intended to model the combustion chamber using a plug flow reactor to capture kinetics, this was decided against due to the complexity of methane combustion modeling that would be difficult to model in Aspen. The RGIBBS reactor was used to achieve chemical equilibrium, and thus maximum conversion of methane. This had the dual effect of lowering natural gas waste out of the product stream and raising CO₂ product purity. As

mentioned earlier, the combustion kinetics are difficult to model using traditional modeling techniques. A methane combustion kinetics package for a software called CHEMKED-II was found that was able to take pressure, composition, and time spent in the reactor as inputs. It then used a series of 325 elementary reactions to model combustion in a batch reactor. By converting the residence time in the batch reactor to residence time in a plug flow reactor, the kinetic model for this plant was developed. The outputs from CHEMKED-II were later used to estimate the combustor volume necessary to reach chemical equilibrium.

Turbine

The turbine design used in this process is based on the configuration and specifications of the turbine used in the 300 MWe and 50 MWe power plant designs made by Allam and the Toshiba Corporation. These turbines were specially designed due to the high temperature and pressure conditions generated by the supercritical CO₂ combustion process. The design for the 50 MWe turbine was constructed and functions properly, serving as confidence that the design for the 600 MWe plant will suit the needs of this project. The single axial gas turbine design has an inlet pressure of 330 bar and a temperature of 1204 °C. Both are relatively high compared to other natural gas turbines. To cope with these conditions, a double shell structure will be used with multiple inner pieces and a solid outer casing which was influenced by existing high pressure steam technology. The temperature will be further managed by utilizing cooling designs such as thermal barrier coatings for the rotor and blades and constructing the base from a nickel alloy which was derived from existing gas turbine technology. The outlet pressure is 30 bar, dictated by a pressure ratio of ten, such that the outlet temperature is 803.49 °C, which is regulated by the maximum temperature the recuperator can handle. The shaft power of the turbine is approximately 797 MWe. Allam elaborates that the development of this design has

made significant advances in its feasibility and cost effectiveness, specifically by being able to deal with significant working fluid in the combustion region, which is a crucial feature of this project.

Recuperator

To get the oxidant and recycle CO₂ streams up to reaction temperature before the combustor, a custom heat exchanger called a recuperator was designed to incorporate the heat produced from the reaction back into the system. In Aspen, the recuperator was modeled as a multi-stream HeatX block where the temperatures in the CO₂ recycle and the CO₂-Oxidant mix are specified, and the temperature of the turbine exhaust stream is not set but determined by the heat balance around the combustion reactor. The recuperator used in the process will be based on the high pressure, high temperature heat exchangers designed by Heatric for the 300 MWe demonstration plant. Heatric was licensed to design the novel recuperator because the strict specifications required are difficult to achieve using conventional heat exchangers on the market. The design uses four stages or blocks for three different streams; the CO₂ recycle, the CO₂-Oxidant mix, and the turbine exhaust. Each stage consists of diffusion bonded plates that form a homogeneous block which allows for parallel or counter-current flow. The first block is constructed from a high nickel alloy such as INCONEL alloy 617 and designed to lower the temperature of the turbine exhaust stream from 700 °C to 550 °C at 300 bar. This alloy has a maximum operating temperature that is between 700 °C to 750 °C. In the final model, the exhaust temperature is 803.49 °C which can be handled by switching the material of construction to a more expensive, higher temperature material such as other high nickel alloys (Zhang et al.,

2018). The other three blocks are made with 316L stainless steel which are designed to cool the exhaust stream to an exit temperature of approximately 60 °C.

Investigation into the design and sizing of the recuperator showed that the use of multiple plate heat exchangers planned for the 300 MWe power plant in Allam (2017) would meet the needs for this 600 MWe power plant with adjustments in scale. The two cold streams, the CO₂ recycle and CO₂-O₂ mix, will run counter-currently to the hot stream, the turbine exhaust for a total duty of 1,133 MW. Specifically, the two cold streams will enter at 62.33 °C and 62.88 °C respectively and both exit at 717 °C. The hot stream will enter at 803.49 °C and exit at 79.24 °C. Although the exhaust stream is entering the recuperator at a slightly higher temperature than Allam and Heatric designed, it is close enough for the equipment to function properly. These temperatures and duties were obtained in Aspen, modeling the recuperator as a multi-stream HeatX block.

The total area for the plate heat exchangers was calculated by finding the area needed for heat transfer between the hot stream to each cold stream and summing them. Using the generic heat transfer equation for a heat exchanger, Equation 3-1, the area can be found based on the Logarithmic Mean Temperature Difference (LMTD), the heat duty, and the overall heat transfer coefficient. The LMTD was calculated from the temperatures for the appropriate hot and cold streams assuming linear slopes using Equation 3-2. Based on *An Introduction to Mass and Heat Transfer* by Stanely Middleman, it was assumed that the overall heat transfer coefficient was mostly affected by the convective heat transfer coefficients and not the conductive heat transfer coefficients, shown in Equation 3-3, as the plates tend to have a relatively small thermal resistance (Middleman, 1997). The convective heat transfer coefficients were calculated using Equation 3-4 which employs values from Aspen and an equation for Nusselt number over a flat

plate under turbulent conditions. The spacing between plates, b , was designated as 3 mm as that is a commonly used value, and the correction factor, F , for plate heat exchangers was set as 1 by Middleman. The Reynolds number was calculated using Equation 3-5, a relationship between mass flow rate and plate width for fluid flowing between plates. Based on pictures and diagrams from the design of the 300 MWe recuperator in Allam, 2017, the width and height of the plates within each block was assumed to be approximately 1 m, which is a reasonable metric based upon other heat exchanger designs. Given the plate thickness of 1.6 mm and plate spacing of 3 mm, there would be approximately 217 plates within a heat exchanger block. Having the viscosity and mass flow rate for each stream from Aspen, the Reynolds numbers and each subsequent variable were found for each stream. The area needed between the exhaust and CO₂ recycle streams was 2,660.66 m², and the area needed between the exhaust and CO₂-O₂ mixstream streams was 1,213.65 m² resulting in 3,874.31 m² total.

Water Separation

The only separation needed for the Allam cycle is water separation which is accomplished using a simple flash drum. The purpose of removing water from the exhaust is to both prevent damage to the CO₂ compressor from entrained liquid and to provide a dry product CO₂ stream for EOR. Additionally, the turbine exhaust must be cooled to a low temperature to increase its density before recompression, which saves on electricity requirements for the compressor. While some of the cooling is done in the recuperator, the process also relies on a condenser before the flash drum to further cool the exhaust. The cooled exhaust from the condenser is then adiabatically expanded in a flash drum such that greater than 99% of the combustion derived water vapor produced in the simulation is removed.

Sizing estimates for the flash drum were calculated using heuristics from Peters, Timmerhaus, and West (Peters et al., 2002). The flash drum was assumed to be a vertical cylinder operating with a mesh deentrainer, which helps knock out entrained liquid water from the cooled exhaust (Couper et al., 2010). A low end Length/Diameter ratio of 2.5 was assumed to keep the overall size of the drum at a minimum. An appropriate gas velocity was calculated using Equation 3-6 using vapor and liquid densities pulled from the Aspen model (Peters et al., 2002). Using the known gas volumetric flow rate from the simulation, a cross sectional area and consequently drum diameter and height were calculated from the L/D ratio. The volume of the drum was found to be large at roughly 1186 m³, although this makes sense due to the scale of the project and its reliance on large recycle flows. To accommodate this volume, the drum would need to have a diameter of approximately 8.5 m and an approximate height of 21.1 m. This size may necessitate multiple flash drum units in parallel. As corrosivity and temperature are expected to be low in this drum, it will be constructed using carbon steel to minimize cost.

Sizing of the condenser before the flash drum was also accomplished through a variety of assumptions. It was assumed that the condenser would be a single shell pass, two tube pass shell and tube heat exchanger with the supercritical CO₂ exhaust on the shell side and the cooling water on the tube side. The cooling water was determined to be appropriate for the tubes since it is the most fouling. Heuristics from Peters, Timmerhaus, and West give estimation overall heat transfer coefficients that are inappropriate for supercritical fluids, which tend to have heat transfer properties intermediate to gases and liquids (Peters et al., 2002). Consequently, an average Nusselt number for supercritical CO₂ was assumed based off of a paper describing heat transfer for supercritical CO₂ (Olson, 2000). Heat transfer resistances from the tubes and the cooling water were assumed to be negligible such that the overall heat transfer coefficient could

be approximated as the internal convective heat transfer coefficient for the supercritical CO₂ (Equation 3-7). A thermal conductivity for the CO₂ was calculated at the average inlet and outlet temperature of the stream using Aspen property modeling. This value was then used to estimate the internal convective heat transfer coefficient using the assumed Nusselt number (Equation 3-8). The LMTD and LMTD correction factors were calculated using Equations 3-2, 3-9, and Figure 3-6. Using the reported condenser heat duty from the Aspen model seen in Table 4-1 in conjunction with Equation 3-10, the heat transfer area was estimated. Using assumptions regarding tube dimensions and Equation 3-11, the number of tubes required was also determined.

The results showed a large heat transfer area of approximately 4446 m² and 4953 tubes, which in practice would necessitate the use of multiple shells. The normal operating pressure in the tube side of the condenser is close to atmospheric pressure as a result of the derivation of cooling water from an ambient cooling tower, while the normal operating pressure of the shell side CO₂ is expected to be 29 barg. As temperatures are relatively low and the cooling water and CO₂ streams are of low corrosivity, the condenser will have a carbon steel construction of both the tubes and the shell.

CO₂ Compressor

Initial design plans employed a simple single stage compressor after the water separation unit to bring the CO₂ product up to the correct pressure of 100 bar to leave the process or be recycled. This increase in pressure leads to a subsequent increase in the temperature. However, this initial design choice was partially preventing the process from achieving a maximum power output. In order to optimize power consumption for the CO₂ compressor, the simple single stage compressor originally included in the Aspen model was substituted with a two stage centrifugal compressor with intercooling. Each stage has an equivalent compression ratio with an intercooler

after the stage to reduce temperature such that a high fluid density is maintained to reduce power consumption. The additional cooling water required for the intercooling serves as a more efficient use of energy compared to the additional work required by a single stage compressor. This compressor was specified to operate at an isentropic efficiency of 0.84, which can be considered the upper bound to supercritical CO₂ centrifugal compression efficiency (Liu et al., 2019). The required fluid power for stage 1 and 2 was found to be 40.4 MW and 32.4 MW, respectively. Intercoolers were assumed to be floating head shell and tube heat exchangers with the CO₂ shell side and the cooling water tube side, and were specified to reduce the temperature of the CO₂ stream to 23°C after each stage of compression. Sizing of the intercoolers was accomplished using the same procedure outlined for the condenser in the water separation section. Intercoolers 1 and 2 require heat transfer areas of 2622 m² and 6855 m², respectively. Intercoolers 1 and 2 also require approximately 2921 and 7636 tubes, respectively. The combination of expected low corrosion rates and temperatures and the need for a relatively high operating pressure range of between 30 to 100 bar warrants that the compressor stages and intercoolers be constructed from carbon steel.

Recycle Pump

Following product CO₂ pull off, there is a centrifugal pump and associated control valve located on the recycle stream to increase pressure to 300 bar. With a pressure difference of 227.01 atm and losses due to length of pipes, friction, and the control valve, the overall differential pressure is 228.34 atm. With a volumetric flow rate of 1.95 m³/s CO₂ passing through the pump, a hydraulic power of 45.12 MW is required to achieve the target pressure. This hydraulic power translates to a supplied shaft power of 64.45 MW based on a 70% shaft efficiency.

Oxidant Pump

To get the oxidant enriched stream up to 300 bar, it must pass through a centrifugal pump and its associated control valve. The oxidant pump faces similar design requirements as the recycle pump; however, the molar flow rate is only 2.5 kmol/s which requires 7.35 MW of hydraulic power to reach the target pressure. Because it also has a 70% shaft efficiency it will require 10.51 MW of electricity to operate. The chosen MOC was carbon steel.

Feed Compressor

The Aspen model was fitted with a feed compressor to more accurately model how the pipeline feed would be converted to match the input requirements of the combustion chamber. The inlet pipeline conditions are 40 bar and 25 °C which is not suitable for injection into the combustion chamber. The feed compressor brings the pipeline up from 40 bar to the required 230 bar for this process. This causes the inlet gas temperature to be raised to 251.65 °C, which is slightly less than what was initially designed by the team. However, this slight drop in the temperature had no impact on the performance of the plant so a heater was not introduced to make up the temperature difference.

3.2.4 Plant Location Choice and Implications

Allam and NET Power decided the optimal location for their 50 MWe demonstration plant was La Porte, Texas. Location is a large factor in the basic economics of a power plant itself as it affects not only the cost of transporting inputs and outputs from the site, but the rates at which these products are sold. To determine the best location for electricity revenue, the largest revenue source for the project, data from the Energy Information Administration (EIA) on

the weighted average wholesale price annualized over the whole year was compared for each of the eight major electricity hubs and their corresponding natural gas trading hubs. Comparing the annual weighted average prices from 2020 provided a more accurate understanding that by choosing the plant site to be California, the price per megawatt-hour increases to the highest option, \$46.45. The annual values better reflect the seasonal changes in electricity usage and subsequently the plant's expected gross revenue than the previously used monthly values. Consequently, this affected the price of the natural gas, which was adjusted to reflect the new supplier at \$0.26 per cubic meter, and the cost of transporting the raw materials and products. The benefit of placing the plant in California is that it would be close to relatively large, operational oil fields such as the Midway Sunset Oil Field shown in Figure 3-3. The close proximity to these oil fields would allow for cheap transfer of the CO₂ product to EOR companies, reducing costs.

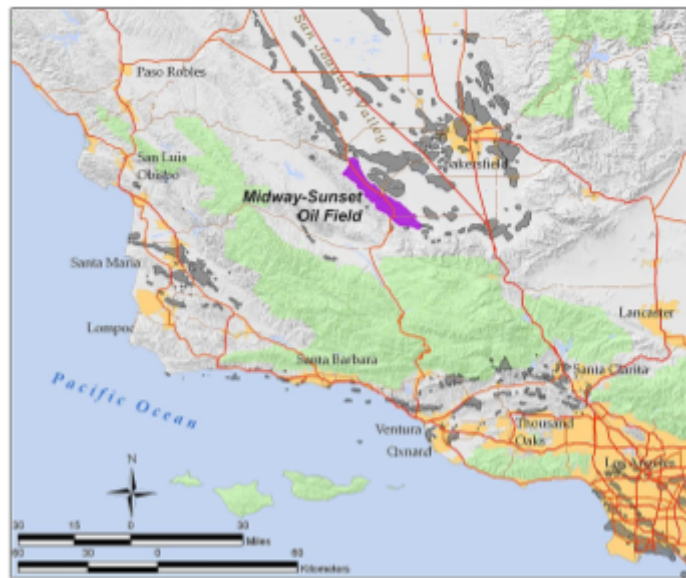


*Figure 3-3: Prospective California Oil Fields
(Midway-Sunset Oil Field, 2021)*

3.2.5 Electricity Utility

Calculations of electricity requirements for various unit operations were performed through the AspenPlus software to provide a basis for electricity consumption in the whole facility. The compressors and pump unit operations all require electric utilities which summed to a 189.79 MW draw as seen in Table 3-2. Unit names are in reference to Figure 4-1.

Table 3-2: Electricity Utility Requirements by Unit Operation

Unit	Usage (MW)
P-101	71.14
T-101	796.64
C-102	86.62
C-101	10.08
C-103	10.51

The turbine (TURBINE) was calculated to produce 796.64 MW of electricity, offsetting the power requirement to a net exported electricity amount of 618.29 MW (Table 3-3). The 178.35 MW of electricity required by the facility as a whole will be supplied by the power generated in the turbine section, thus giving a net quantity of electricity to be sold as a product. The net product of electricity is 618.29 MW and is greater than the target amount and thus the project does meet the intended specifications of the project design.

Table 3-3: Net Electricity (MW)

Generated	796.64
Consumed	178.35
Net Total:	618.29

3.2.6 Cooling Water Utility

In order to satisfy the cooling requirements of the CO₂ compressor and the water separation condenser, a cooling water utility had to be developed in the simulation. E-102 and C-102 have heat duties amounting to 432 MW. Because cooling towers operate off of evaporative cooling, they can realistically achieve cooling water temperatures that are 2°C above the ambient wet bulb temperature (*Wet Bulb Temperatures and Cooling Tower Performance | Delta Cooling Towers, Inc.*, 2017). According to cooling tower heuristics, it is also appropriate to operate the cooling tower in this project with a range of 8.3°C (*Cooling Tower Efficiency*, n.d.). Typically, the maximum relative humidity of ambient air coincides with the lowest dry bulb temperature of the air in a given day and vice versa. Dry bulb temperature and relative humidity data for each day were analyzed over the year 2020 in Kern county, which is a county in close proximity to the largest California oil field (*California Weather Data: Formatted Report--UC IPM*, n.d.). A wet bulb temperature formula, seen in Equation 3-8, was used to determine the maximum wet bulb temperature of 2020, and this temperature was taken as the worst case operating scenario for cooling (*Wet Bulb Calculator*, n.d.). Similarly, an average and best case wet bulb temperature was calculated. Table 3-4 highlights the resulting operating cases and their cooling water requirements.

Table 3-4: Cooling Water Operating Cases and Specifications

Case	Wet Bulb Temperature (°C)	Cooling Tower Outlet Temperature (°C)	Cooling Tower Inlet Temperature (°C)	Cooling Water Requirements (kg/s)
Best	-5.6	1.0	9.3	14,417
Average	11.3	13.3	21.6	14,484
Worst	24.5	26.5	34.8	N/A

Table 3-4 shows that when operating with a low wet bulb temperature, the cooling tower can achieve lower temperatures through ambient cooling such that cooling water requirements are slightly reduced compared to the average operating case. This leads to a slight increase in process efficiency since less cooling water and associated cooling loop operation costs are required. The worst case scenario is problematic for this process because at a temperature of 26.5°C, cooling water can no longer be used in the condenser and CO₂ compressor intercoolers due to a temperature crossover. There are a few potential options that would allow for operation during this case. The first option would be to employ an onsite backup chiller that can produce chilled water at low enough temperatures to avoid a crossover. Another possibility is that a throttling valve could be used to add a small pressure drop to the process to accomplish additional required cooling. Both of these options lead to decreased process efficiency and worse economics and are therefore undesirable. The final option is to suspend plant operation during days where the wet bulb temperature is too large - this does not affect process efficiency but leads to additional downtime and less yearly revenue.

3.2.7 Difficulties in Design

To model the large-scale natural gas Allam cycle (600 MWe), process conditions achieved in the Allam cycle pilot plant project, such as electrical and thermal efficiencies and stream conditions such as temperature and pressure, were used as a basis for initial Aspen modeling. The simulation was broken up into simple steps to ensure convergence could be easily identified. To establish the overall mass balance for the process, stream conditions were initially ignored in favor of specifying combustor and water separator temperatures and pressures. Initially, the model was set up using only equipment important for the material balance such as splitters, the combustor, and the flash drum. Setting up the simulation in this manner easily

allowed for the specification of a recycle stream and achieved convergence while still maintaining an accurate material balance. Based on error messages and past modeling experience, it was determined that the most likely source of convergence error was involving the tear stream for the recycle process. To assist in getting the model to converge, the recycle stream flow was specified rather than the split fraction, and the product stream flow rate was allowed to float. Additionally, the recycle stream was explicitly specified as a tear stream. In changing these two aspects, convergence was achieved for the simplified material balance model. After this step, all other unit ops, which were mostly those affecting stream temperatures and pressures like compressors/turbines, heaters/condensers, and the recuperator, which was modeled as a multi-stream heat exchanger, were added to the simulation. Convergence was then achieved by tweaking some process conditions away from Allam 2017 as discussed below.

Operating the simulation at the same fuel-air ratio as in Allam 2017 resulted in too low a CO₂ outlet purity. By increasing the oxygen flow rate from 2.11 kmol/s to 2.17 kmol/s, the fuel-air ratio was moved closer to stoichiometric away from fuel rich combustion. As a result, the product CO₂ purity was able to reach 90 mol%, which is the minimum requirement for enhanced oil recovery.

Utilizing the same split fraction for the oxidant-CO₂ stream and the same oxygen flow rate as in Allam 2017 posed a challenge regarding stream phases in the Aspen model. A high amount of vapor was initially present in the CO₂-oxidant stream - to combat this, the supercritical oxygen flow rate (16°C and 100 bar) was increased to 2.2 kmol/s from 2.17 kmol/s. This also had the effect of increasing product CO₂ purity to 95 mol%. As initially modeled, the oxygen flows into the system and mixes with roughly 22% of the recycle stream pulled off to form a CO₂-oxidant stream as done in Allam 2017. Even after increasing the oxygen flow rate,

the CO₂ diverted to the oxidant stream was not enough to bring the stream to a liquid state that the pump is capable of handling. To address this phase issue, the CO₂ pulled off for the oxidant stream was increased to 47.5% of the recycle stream by specifying flow rate, allowing for a liquid inlet to the pump.

After solving these simulation issues, both the combustor and the water separator (modeled as a flash drum at this point), were changed to operate adiabatically with zero pressure drop. This alteration did not hinder convergence and moved us a step closer to properly modeling the power cycle. At this stage, it was believed that there was no longer enough CO₂ quench stream flow to keep the reaction temperature low enough for the turbine specs. Future improvement steps may be to bring oxygen in at a different condition so that less CO₂ will be needed for the oxidant stream, or to draw off slightly less CO₂ product to increase the overall recycle flow rate.

C-101	R-101	R-102	T-101	E-101	E-102	V-101	C-102	P-101	C-103
Pipeline Fuel Compressor	Combustion Chamber - First Half	Combustion Chamber - Second Half	Turbine	Recuperator	Pre-Water Separation Cooler	Water Separation Flash Drum	Multi-Stage Compressor with Intercooler	CO ₂ Recycle Pump	O ₂ Compressor

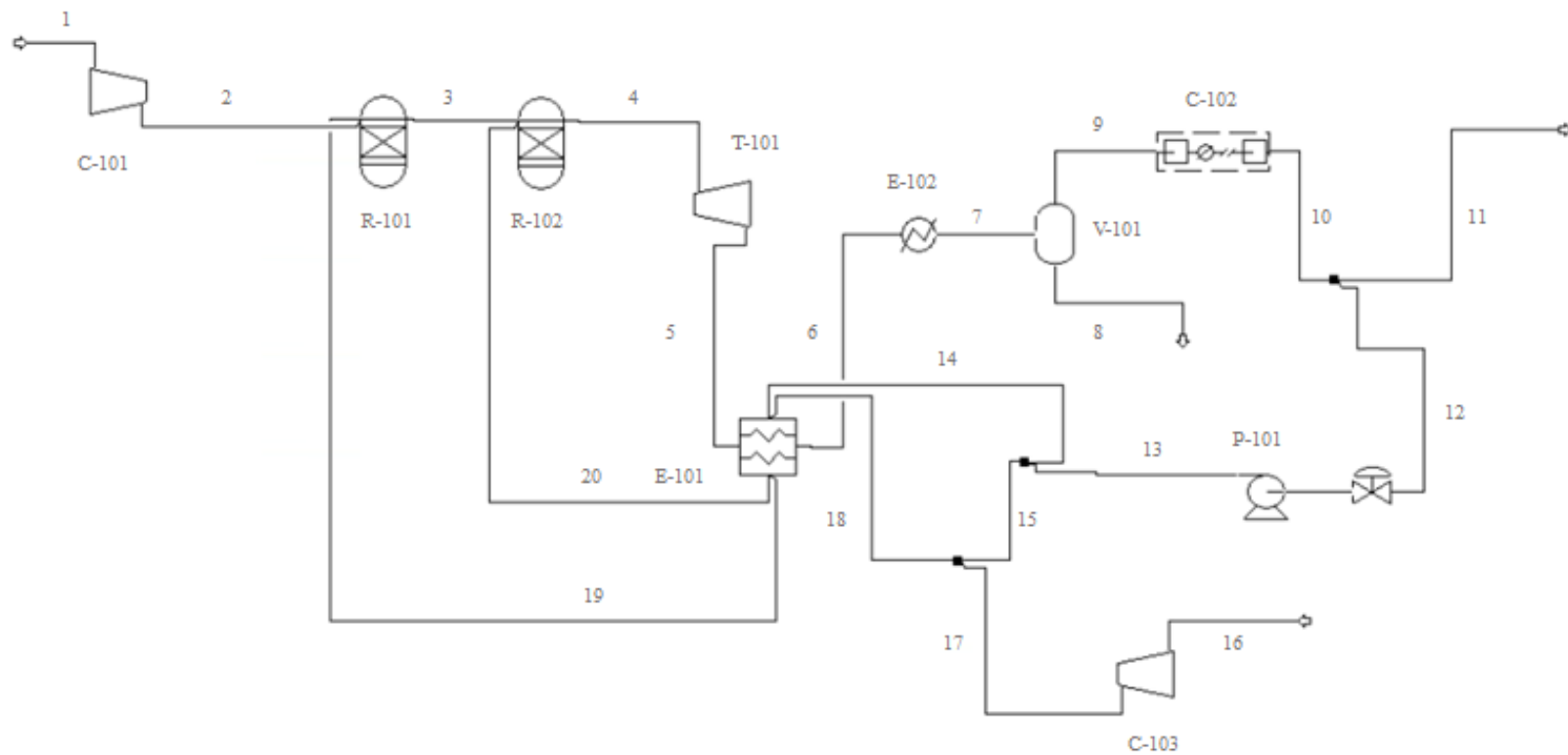


Figure 4-1: Process Flow Diagram and Legend

4. Final Recommended Design

4.1 Process Flow Diagram

The current process flow is shown in Figure 4-1. It operates in a similar manner to the process description of the Allam cycle given earlier, but has a few key modifications to help optimize performance. It starts with taking the pipeline natural gas and compressing it to be in line with the high pressure end of the cycle. This compression also heats the vapor to the point that when injected into the combustion chamber, the flame will remain stable. This is an important step because the natural gas and a recycle stream of O_2 that is heavily diluted with CO_2 is passed through the combustion chamber. Another, oxygen deficient CO_2 stream is injected into the combustor about halfway through the length of the chamber to quench the outlet stream. The exhaust from the combustion chamber is passed through the turbine where it is expanded from 330 bar to 30 bar. The expansion also results in a temperature decrease which cools the exhaust stream to the point that the recuperator material can handle. The recuperator takes the heat from the exhaust stream and distributes it to the oxygen enriched CO_2 stream and the quenching CO_2 stream. After passing through the recuperator, the cooled stream is passed through a cooler and then into a flash drum. The flash drum separates out enough water that it can be sold for EOR. The resulting vapor stream is passed through a compressor before a fraction of it is taken off as the product stream to be sold for EOR. After the product stream is taken off, it is split into two streams. One of those streams will be mixed with the O_2 stream coming from the ASU. Both streams pass through the recuperator and go back into the combustor to complete the cycle.

4.2 Equipment Tables and specifications

Table 4-1. Shell and Tube Heat Exchanger Specifications

Unit	Heat Duty (MW)	Tube/Shell Fluid	Tube/Shell MOC	Heat Transfer Area (m²)	Number of Tubes	Bare Module Cost
E-102	128	CW/CO ₂	CS/CS	4446	4953	\$3,050,000
C-102 Intercooler 1	96	CW/CO ₂	CS/CS	2622	2921	\$1,890,000
C-102 Intercooler 2	278	CW/CO ₂	CS/CS	6855	7636	\$5,300,000

* Tube dimensions of 15 m length, 19.05 mm outer diameter, and 16.56 mm inner diameter

Table 4-2. V-101: Flash Drum Specifications

Inlet Pressure (bar)	Diameter (m)	Height (m)	Volume (m³)	MOC	Demister MOC	Bare Module Cost
30	8.45	21.1	1186	CS	SS	\$33,400,000

Table 4-3. R-101 and R-102: Combined Combustor Specifications

Residence time (s)	Diameter (m)	Height (m)	Volume (m³)	MOC	Bare Module Cost
0.26	1.24	2.48	2.99	Nickel	\$242,000

Table 4-4. Turbine, Compressor, and Pump Specifications

Unit	Inlet Pressure (bar)	Pressure Ratio	Type	No. Spares	MOC	Bare Module Cost
T-101	330	0.09	Axial	0	Nickel	\$14,100,000
C-101	40	8.25	Centrifugal	1	CS	\$12,900,000
C-102	30	3.33	Centrifugal	0	CS	\$56,800,000
C-103	100	3.30	Centrifugal	1	CS	\$13,300,000
P-101	100	3.30	Centrifugal	1	CS	\$124,200,000

Table 4-5. E-101: Recuperator Specifications

Heat Duty (MW)	Tube Pressure (bar)	Type	MOC	Area (m²)	Number of Plates	Bare Module Cost
1133	330	Flat plate	Nickel/Stainless steel	3874	217	\$8,580,000

4.3 Material and Energy Balances

Table 4-6: Stream Table for Streams 1-5

Stream Number		1	2	3	4	5
Temperature (°C)		25.00	235.19	1980.10	1204.18	803.07
Pressure (bar)		40	330	330	330	30
Mole Flows (kmol/sec)		1.25	1.25	13.09	34.73	34.73
Mole Fraction	H₂	0.00	0.00	0.00	0.00	0.00
	N₂	0.02	0.02	0.01	0.01	0.01
	O₂	0.00	0.00	0.01	0.00	0.00
	CO	0.00	0.00	0.01	0.00	0.00
	METHANE	0.95	0.95	0.00	0.00	0.00
	ETHANE	0.03	0.03	0.00	0.00	0.00
	CO₂	0.01	0.01	0.79	0.91	0.91
	PROPANE	0.00	0.00	0.00	0.00	0.00
	WATER	0.00	0.00	0.19	0.07	0.07

Table 4-7: Stream Table for Streams 6-10

Stream Number		6	7	8	9	10
Temperature (°C)		79.24	17.00	17.00	17.00	23.00
Pressure (bar)		30	30	30	30	100
Mole Flows (kmol/sec)		34.73	34.73	2.48	32.26	32.26
Mole Fraction	H₂	0.00	0.00	0.00	0.00	0.00
	N₂	0.01	0.01	0.00	0.02	0.02
	O₂	0.00	0.00	0.00	0.00	0.00
	CO	0.00	0.00	0.00	0.00	0.00
	METHANE	0.00	0.00	0.00	0.00	0.00
	ETHANE	0.00	0.00	0.00	0.00	0.00
	CO₂	0.91	0.91	0.00	0.98	0.98
	PROPANE	0.00	0.00	0.00	0.00	0.00
	WATER	0.07	0.07	1.00	0.00	0.00

Table 4-8: Stream Table for Streams 11-15

Stream Number		11	12	13	14	15
Temperature (°C)		23.00	23.00	60.90	60.90	60.90
Pressure (bar)		100	100	330	330	330
Mole Flows (kmol/sec)		1.29	30.97	30.97	21.68	9.29
Mole Fraction	H₂	0.00	0.00	0.00	0.00	0.00
	N₂	0.02	0.02	0.02	0.02	0.02
	O₂	0.00	0.00	0.00	0.00	0.00
	CO	0.00	0.00	0.00	0.00	0.00
	METHANE	0.00	0.00	0.00	0.00	0.00
	ETHANE	0.00	0.00	0.00	0.00	0.00
	CO₂	0.98	0.98	0.98	0.98	0.98
	PROPANE	0.00	0.00	0.00	0.00	0.00
	WATER	0.00	0.00	0.00	0.00	0.00

Table 4-9: Stream Table for Streams 16-20

Stream Number		16	17	18	19	20
Temperature (°C)		16.00	157.71	62.35	717.00	717.00
Pressure (bar)		100	330	330	330	330
Mole Flows (kmol/sec)		2.50	2.50	11.79	11.79	21.68
Mole Fraction	H₂	0.00	0.00	0.00	0.00	0.00
	N₂	0.00	0.00	0.01	0.01	0.02
	O₂	1.00	1.00	0.21	0.21	0.00
	CO	0.00	0.00	0.00	0.00	0.00
	METHANE	0.00	0.00	0.00	0.00	0.00
	ETHANE	0.00	0.00	0.00	0.00	0.00
	CO₂	0.00	0.00	0.77	0.77	0.98
	PROPANE	0.00	0.00	0.00	0.00	0.00
	WATER	0.00	0.00	0.00	0.00	0.00

4.4 Process Economics

4.4.1 Capital Costs

The capital cost of the equipment was estimated using a Chemical Engineering Plant Cost Index (CEPCI) of 560 which served as an estimate for the CEPCI of the 2018 fiscal year. The cost of every major and ancillary piece of equipment was estimated using equations and relationships provided by Turton et al. as Allam and Heatric published no financial statements from which to base estimates (Turton et al., 2018). The costs for the smaller compressors, C-101 and C-103, were scaled based on designs needing 8067 kW and 8411 kW of fluid power respectively in addition to accounting for a spare compressor. The larger compressor for the CO₂ recycle stream, C-102, required 72764 kW of fluid power split between two stages in addition to two shell and tube heat exchangers to function as intercoolers between the stages. As this compressor is significantly larger than the others no spare was designed into the process. The compressors and the turbine, T-101, are all rotary pieces of equipment and must be designed with the vendor, such as Heatric or Toshiba, to most accurately determine the cost. The flat plate recuperator, E-101, was cost estimated based on using a nickel alloy material of construction (MOC) for the first of four blocks and a stainless steel MOC for the last three blocks, all of equal area, 969 m², per block. The water separator flash drum, V-101, was modeled as a cylindrical, vertical container with the appropriate length and diameter using a carbon steel MOC. The cost for the CO₂ recycle stream pump, P-101, was estimated needing 64500 kW, having a carbon steel MOC, and accounting for one spare. The complete pricing factors, module costs, and base equipment costs for each piece of equipment are shown in Appendix 10.5. The estimates for the purchased equipment costs sum to \$57,893,500 as shown in Table 4-10.

Table 4-10: Purchased Equipment Costs

Unit	Purchased Equipment Cost (\$)
C-101	4,720,000.00
C-102 Stage 1	11,500,000.00
C-102 Stage 2	9,180,000.00
C-102 Intercooler 1	632,000.00
C-102 Intercooler 2	1,870,000.00
C-103	4,850,000.00
R-101	30,300.00
R-102	30,300.00
T-101	4,039,900.00
E-101	2,750,000.00
E-102	978,000.00
V-101	17,000,000.00
P-101	313,000.00
	<hr/>
	57,893,500.00

The total capital cost for the plant (FCI) was estimated using the Lang approximation, where the sum of purchased equipment costs is multiplied by the lang factor (Turton et al., 2018). For a fluid processing plant such as this, the lang factor is 4.74. Therefore, the FCI was estimated to be \$274,400,000. The current design is a class four design such that approximately one to fifteen percent of the project is defined (Turton et al., 2018). The current design is of average economic estimation risk as it uses both novel and standard technology, which is harder and easier to estimate respectively. The design is also at average risk because although it is a relatively new process for natural gas based energy production, natural gas power plants are not new design projects. Therefore, this class four design would be of average economic risk for a company with previous power plant design experience to estimate financially, and the plant capital costs could range from 148% to 68% of the calculated FCI. The actual total plant capital costs could be between \$406,112,000 and \$185,592,000.

4.4.2 Operational Costs

The power plant's basic economics for inputs and outputs are based on how much of the year the plant is able to run and whether it can produce the theoretical maximum capacity while in operation. Additionally, the power plant is affected by demand from the electrical grid. Given that the plant plans to operate for almost the entire year, the electrical grid demand is the strongest indicator of the plant's production schedule. Differing demands on the grid and cooperation with other power sources lower the actual output of the plant. The demand on the electrical grid peaks shortly in the morning and largely in the evening, while a lull in the middle of the day reduces the maximum capacity (*California ISO - Today's Outlook, 2021*). The production of natural gas power plants also decreases during daytime hours due to solar power filling most of the demand. A metric by which all of these factors can be quantified is the capacity factor, which measures the actual annual output of the power plant as a percentage of the theoretical annual output if the plant were operating at maximum capacity 24 hours a day, 365 days a year. The capacity factor for our plant was determined to be 57.3% (EIA, n.d.).

Our power plant requires inputs of natural gas and pure oxygen gas. Data on commercial prices of oxygen gas proved difficult to obtain for this project due to a large industrial-scale demand while most oxygen is sold to labs in small canisters. Obtaining data for natural gas prices was also difficult. No public data was found through and retrieving this data from company representatives also proved unsuccessful. Eventually, the Enbridge company, a supplier to both Canada and the northeastern United States, released information regarding their prices for pipeline quality natural gas as well as its composition. The natural gas is therefore priced as if it were sourced from the Enbridge company. An industrial contract is needed as the plant requires more than 2400 m³ daily. Hourly consumptions were converted to annual consumptions based on hours and then to actual consumption by multiplying by the capacity factor of the plant, 57.3%.

Table 4-11: Input Costs per Year

Input Item	Amount per Year	Cost per Unit	Total Cost per Year
Oxygen	1.446 billion kg/yr	0.07 \$/kg	\$101,188,852
Natural Gas	380.64 million kg/yr	0.009 \$/kg	\$3,423,390
Total:			\$104,612,242

According to Turton, the number of operators needed at one time can be calculated from Equation 4-1, which is the Alkhayat and Gerrard correlation (Turton et al., 2018). This process has no particulate processes as every input and output are pipelines and no particulate removal is included. There are nine non-particulate unit operations, therefore Eq. 4-1 shows that 2.89 operators are needed at any one time. Turton also recommends that 4.5 operators are hired for each operator needed in the plant (Turton et al., 2018). These values indicate that 13.005 operators need to be hired, which is rounded up to fourteen. The United States Bureau of Labor Statistics states that the average chemical operator in California makes \$54,330.00/year in wages (Bureau of Labor Statistics, 2021b). The Bureau also states that wages make up approximately 70% of a total salary package as benefits are the other 30% (Bureau of Labor Statistics, 2021a). With all of this information, the total annual operational labor cost was calculated to be just over one million dollars as seen below.

Table 4-12: Operational Labor Costs per Year

Operators Hired	14
	\$ Amount/yr
Annual Operator Wages	\$54,330.00
Total Annual Salary (With Benefits)	\$77,614.29
Total:	\$1,086,600.00

Required utilities are electrical and cooling water. The electrical utilities are supplied through the on-site turbine so this cost is \$0 per year. Cooling water utilities are used by the heat exchangers (E-102 and C-102). This usage is corrected by the capacity factor from a theoretical usage to an actual usage. The total annual utility cost of the plant is detailed below.

Table 4-13: Utility Costs per Year

Unit	Duty (MW)	Usage (kg/hr)	\$/hr	\$/year
E-102	128	7,322,941.96	\$97.69	\$490,350.17
C-102	373.90	21,391,000.00	\$285.36	\$1,432,358.82
Total:			\$383.05	\$1,922,708.99

The plant outputs all of its waste to the environment in a safe and sustainable manner such that the waste treatment cost of the plant (C_{WT}) is \$0 per year. With capital costs (FCI), raw materials (C_{RM}), operational labor (C_{OL}), waste treatment (C_{WT}), and utilities (C_{UT}) all known, the standard cost of manufacturing (C_{OM}) can be calculated. The C_{OM} includes the previous expense categories, but also other items related to upkeep, taxes and dues, and non-operational labor. Table 4-14 details these line items, their estimation given by Turton, and the resulting cost (Turton et al., 2018). Depreciation is calculated on a 10% straight-line analysis, which is an oversimplified case of operating the plant for ten years. The resulting total cost of \$216,503,087 is regarded as the total expenditure of the plant for one calendar year.

Table 4-14: Standard Cost of Manufacturing Breakdown and Estimation per Year

Cost Type	Cost Item	Estimation	Total Costs (\$/yr)
Direct Costs	Raw Materials	C_{RM}	\$104,612,242
	Waste Treatment	C_{WT}	--
	Utilities	C_{UT}	\$1,922,709
	Operating Labor	C_{OL}	\$1,086,600
	Direct Supervision and Clerical Labor	0.18 C_{OL}	\$195,588
	Maintenance and Repairs	0.06 FCI	\$16,464,000
	Operating Supplies	0.009 FCI	\$2,469,600
	Laboratory Charges	0.15 C_{OL}	\$162,990
	Patents and Royalties	0.03 C_{OM}	\$6,325,092
Fixed Costs	Depreciation	0.1 FCI	\$27,440,000
	Local Taxes and Insurance	0.032 FCI	\$8,780,800
	Plant Overhead	0.708 C_{OL} + 0.036 FCI	\$10,647,713
General	Administration Costs	0.177 C_{OL} + 0.009 FCI	\$2,661,928
Manufacturing	Distribution and Selling Costs	0.11 C_{OM}	\$23,192,005
Expenses	Research and Development	0.05 C_{OM}	\$10,541,820
Total:			\$216,503,087

4.4.3 Revenues

Electricity is the largest source of income for the power plant and can be sold to local power companies at the below estimated rate. The effluent mixed stream with mostly CO₂ has many applications. The relative costs of selling the product for EOR, sequestering it in the ground, or selling it for commercial use were considered before a decision was made. It was determined that the best course of action was to sell the CO₂ stream for EOR. This decision was reached through applying the project goals (prevent CO₂ release to the atmosphere) and

economics (no capital cost or operating cost compared to sequestration). Selling for EOR does have an economic tradeoff in that the power plant cannot claim tax credits for the CO₂; these credits would go to the EOR company. The annual electricity and CO₂ outputs are converted to actual outputs through the capacity factor of 57.3% which reduces the overall output. The selling price and annual income from the CO₂ product is observed below.

Table 4-15: Output Income per Year

Output Item	Amount per Year	Income per Unit	Total Income per Year
Electricity	3.103 million MWh/yr	46.45 \$/MWh	\$144,157,310
CO ₂	1.02 million metric ton/yr	40.00 \$/metric ton	\$40,786,140
Total:			\$184,943,450

4.4.4 ROI

Summing the capital and operational costs with the revenues shows that this plant, with current design and economic estimates, would produce a financial loss of \$4.12 million annually when in full operational capacity. This is seen in Table 4-16.

Table 4-16: Annual Return on Investment

Economic Impact	Annual Total
Cost of Manufacturing	\$216,503,087
Product Income	\$184,943,450
Taxable Profit	\$31,559,637
Income Tax	\$0
Depreciation	\$27,440,000
After-Tax Cash Flow	\$4,119,637

However, changes in the prices of the raw materials and products can change the overall economics of the plant. For instance, if the wholesale price of electricity increased from the average \$46.45 / MWh to \$47.78 / MWh, the product income would increase to \$189,063,087 per year. This whole price of electricity would offset the cost of manufacturing, and any price at that value or higher would make the plant profitable. Additionally, a decrease in the cost of oxygen from a change in economic pricing or the development of an in-project ASU would lower the cost of manufacturing. Decreasing the cost of oxygen from \$0.07 / kg to \$0.067 / kg would lower the cost of manufacturing to \$212,383,450 per year, thus making the plant profitable. Any lower price would also increase the plant's profitability. Because the plant does not currently earn money, ROI analyses would yield unhelpful results. The above break-even scenarios would prevent the accrument of debt, but would not pay off the fixed capital investment or earn money. The design suggestions found in Section 6 offer routes to possible profitability and ROI with further work.

5. Safety, Health, and Environmental

5.1 Material Compatibility

Y : Compatible
N : Incompatible
C : Caution
SR : Self-Responsive
 * : Changed by user

NFPA				Allam Cycle Compatibility Chart	CARBON DIOXIDE	CARBON MONOXIDE	ETHANE	METHANE	NITROGEN	OXYGEN	PROPANE
Health	Flammability	Instability	Special								
				CARBON DIOXIDE							
3	4	0		CARBON MONOXIDE	Y						
1	4	0		ETHANE	Y	Y					
2	4	0		METHANE	Y	Y	Y				
				NITROGEN	Y	Y	Y	Y			
3	0	0	Oxi	OXYGEN	Y	N	N	N	Y		
2	4	0		PROPANE	Y	Y	Y	Y	Y	N	

Figure 5-1: Component Compatibility Chart describing potential reactive hazards

To determine reactive hazards in the process, a component compatibility was performed with the American Institute of Chemical Engineers' (AIChE) Chemical Reactivity Worksheet (CRW) program. The results of the report seen above in Figure 5-1 indicate reactive hazards between oxygen and the hydrocarbons present in the process. This result is expected and relied upon as this is a combustion based process, however this does inform that this reaction occurs spontaneously and the components must be carefully contained until their intended mixing.

Furthermore, this study highlights the fact that most all of these components have a high flammability and health hazard risk.

5.2 Credible Events

5.2.1 Loss of Primary Containment

Loss of primary containment (LOPC) events occur as an unplanned or uncontrolled chemical release from primary containment (AIChE, 2014). Both toxic and non-toxic chemicals are included in this category. In this process design, LOPC would occur through rupture of pipelines or unit operations rather than from a storage area as the proposed design brings reactants in at continuous steady state and removes them from the process in the same manner. Equipment rupture could occur through two routes; either an overpressure on the inside of the equipment which leads to mechanical failure, or a chemical effect on the material of construction which results in a compromised mechanical strength. The former of these two options is discussed in more detail in the section below.

Our methane and oxygen flows into the process are non-corrosive to both aluminum and carbon steel so chemical processes leading to mechanical strength failure are not anticipated (Government of Canada, 2021). Carbon dioxide, carbon monoxide and water can combine to create an atmosphere where stress corrosion cracking (SCC) can occur at temperatures below the dewpoint (EIGA, 2004). It is possible that the process will be operating beneath the dew point at various times so corrosion might occur. While this situation is not anticipated often, the hazard should be made known to ensure human safety in the vicinity of the project. Sensors and monitors will be placed, regularly inspected, and kept up to date on piping and any unit after the recuperator in the loop that contain this mixture to accommodate changes in the site's weather conditions. Exchanging of equipment and piping after the combustor is recommended to prevent

corrosion issues from taking hold and eventually leading to mechanical failure and chemical release.

A LOPC incident in the combustion unit would cause an uncontrolled fire and could result in temperature fluctuations or increased pressure in other areas of the process. A LOPC in any area necessitates a shutdown of the plant to limit fire hazard and plume dispersions.

5.2.2 Temperature Fluctuations

Temperatures in this process vary wildly in the different unit operations, ranging from approximately room temperature (17-25°C) to extremely hot regions in the combustor (~2,000°C). While construction materials are being chosen to accommodate these extreme environments, it should not go unobserved that there is always potential for these units to have temperature fluctuations. These fluctuations could lead to undesired phase changes or increases in pressure. An increase in pressure could also lead to LOPC ruptures or to an increase in flow rates through the system. Flow rate increases as a result of temperature fluctuations can lead to adverse process effects such as destabilizing the combustion flame.

If loss of cooling occurs, increasing flow to the combustor, this can lead to non-ideal combustion which would introduce unreacted reactants to later unit operations and create unsafe operating conditions. If cooling cannot be restored quickly, a facility lockdown must be initiated to prevent runaway conditions from developing and threatening the integrity or safety of the project. Loss of cooling shutdowns should remain in effect until the cause of the cooling loss can be identified and corrected to ensure personnel safety during diagnosis and maintenance.

Post-recuperator temperature decreases create the potential for the CO₂ stream to leave a supercritical fluid phase and become liquid. This phase change creates vulnerabilities should a pipeline rupture occur and cause a rapid phase change to vapor and a resulting overpressure.

Temperature decreases in this area of the process should be monitored closely and returned to normal conditions as soon as possible. Shutdowns are unnecessary however. Temperature increases are not as concerning on this side of the process as one stream is a supercritical fluid and the other is water that exits the process to an evaporation pond. Sensors will be placed on all pipelines and unit operations to allow operators direct monitoring and control over the temperatures in the process.

5.2.3 Pressure Fluctuations

Pressure fluctuations are largely the result of temperature fluctuations, flow rate fluctuations or equipment failures. Overpressures on the inside of a piping system or unit operation that result in a large enough pressure differential against the atmosphere will cause the mechanical integrity of the equipment to fail which will lead to a LOPC incident as seen in later sections. Pressure indicators should be present on piping systems and unit operations to ensure that operators are informed about the state of processes on site and be able to maintain control over the process through cooling water, stream flow rates and input/output stream flow rates. Pressure relief devices should also be installed on the combustor, flash separator, and on the recycle loop stream before it rejoins with the oxygen stream to keep the process running as it should. Given the unlikely nature of such events and relatively low toxicity of the chemicals involved, venting to the atmosphere at heights above 20 meters will prevent adverse health or environmental effects from occurring such as carbon monoxide poisoning, according to the ALOHA software (US EPA, 2013).

5.2.4 Process Flow Fluctuations

Process flow fluctuations can be the result of fluctuations of incoming reactants (natural gas and oxygen gas from outside companies). So long as waste stream specifications are being met, safety concern is low even though production may not be at peak times. Should large increases or decreases occur in flows inside the process, it should be determined whether a LOPC incident has occurred. If the flows of input or output streams fluctuates in an uncontrolled manner, contact should be made with the companies giving and receiving these streams to coordinate response.

5.2.5 Explosions and Flammability

This process makes use of methane combustion in a controlled manner as the primary change-in-energy process. While the plant is designed to operate safely, with high strength MOC and a lack of on-site storage of explosive and flammable materials, fire hazards are still prevalent and must be dealt with. Most notably, methane is the primary species in the natural gas feed coming into the plant. Methane is readily flammable and a mild asphyxiant as indicated by the National Fire Protection Association's fire diamond for methane, displayed in Figure 5-2 (PubChem, n.d.). A numerical ranking of four indicates extreme hazard while lower numbers indicate lower hazard levels. The red diamond is for fire hazard, blue is for health, yellow is for stability, and white is a special indicator.

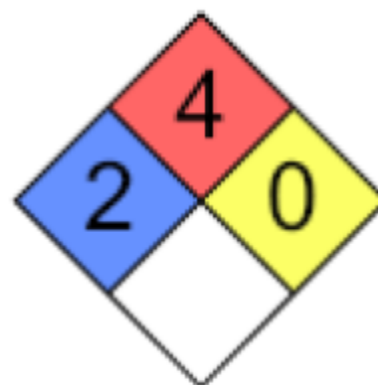


Figure 5-2. NFPA Diamond for Methane

Beyond the passive hazard of methane, methane ought to be considered in its active scenario. Because the feed going into the combustor is 95mol% methane and 0mol% O₂, the

stream is above methane's upper flammability limit of 15% methane in air by volume (PubChem, n.d.). After the combustor, there is no leftover oxygen or methane. Therefore, the combustion can only occur in the combustor and is the only location worthy of intense flammability precautions. All pipelines going in and out of the combustor as well as the surrounding area ought to be protected in the event of a large rupture or combustion occurring in pipelines. This could occur if sufficiently high temperatures are present in the combustor feed streams and contamination occurs (oxygen or natural gas enters the wrong pipeline due to other equipment failures). Should an uncontrolled release or combustion occur, it would be classified as a jet fire since the process is continually running. Pool fires are not a concern as there are no flammable liquids in this process.

To prevent unexpected ignition, all electrical equipment in the area ought to be stored in explosion-proof housing. Additionally, ensuring proper grounding and bonding for equipment and unit operations will prevent the buildup of static electricity which will prevent internal explosions in undesired areas. Sprinkler systems also ought to be implemented in the immediate area to quickly mitigate any hazardous escapes. Emergency shutoff valves for both the incoming oxygen and natural gas feeds should be placed on-site away from the combustor to cut off fuel in the case of an emergency. Inerting the process with CO₂ as a working fluid greatly reduces the possibility of fire or explosion hazard.

5.3 Modeling of Release

The use of dispersion modeling software was used to gain an accurate sense of the potential scenarios that a loss of primary containment could press upon the general public. While these modeling scenarios do not accurately predict any and all scenarios a release could cause,

they employ many aspects that could affect plume dispersion such as weather, terrain, the type and size of release, the specific chemicals released, and site location (Unnerstall, 2021). The EPA has released to the public domain the ALOHA (Areal Locations of Hazardous Atmospheres) software as part of the CAMEO (Computer-Aided Management of Emergency Operations) suite (US EPA, 2013). ALOHA takes into account the climate conditions of a release, the location, the chemical released, and the condition of release (pipeline, puddle, tank, etc.) to model a plume release and to indicate where concentrations are above safety thresholds. ALOHA may work in tandem with another CAMEO software package, MARPLOT, which can plot the plume on top of a digital map to give real life locations. MARPLOT uses Google Maps as its basis by default (US EPA, 2013).

To demonstrate how the software is able to give accurate models for emergency responders to use in the event of a release, a case study was developed and modeled. This case study modeled the release of different chemicals from different points in the system. Most notably, the case study deals with pipeline ruptures in the CO₂ effluent stream and the natural gas input stream. Releases of natural gas, hydrogen gas (H₂), carbon monoxide, and carbon dioxide all received individual models as ALOHA can only model one chemical plume release at a time. ALOHA used the site location as approximately in Bakersfield, California. Weather data was obtained from average weather data for Bakersfield, California and inputted to the model (Weather Spark, n.d.). Bakersfield was selected to retrieve weather data from due to its close proximity to the Midway Oil Fields and appearance in the ALOHA databank. The weather data is specifically modeled on late April, early May average data. While wind, cloud, and temperature changes occur throughout the year, this time of year was chosen to accommodate some of the worst case scenarios with high wind speeds, high temperature, and low cloud cover.

All concentration measurements are made for approximately three meters above the ground. Characteristics for pipeline diameter and length were obtained from a published review of operational U.S. CO₂ and natural gas pipelines (ArcGis, 2021; NaturalGas.org, 2013; Peletiri et al., 2018). All of the data inputted to the model is listed in Table 5-1 below. Data specific to one model (such as pipeline conditions) are listed in Table 5-2 and Table 5-3 and followed by their respective ALOHA model in Figure 3 and 4. Table 5-2 was used for models involving CO and H₂ gas releases and Table 5-3 was used for modeling the input natural gas pipeline. It should be noted that the risk posed by a CO release is much greater as the scale is on the order of miles, not yards. While no residential communities are in danger based on current oil field siting, over-the-fence hazards should be communicated to surrounding operations. Since CO₂ is a supercritical fluid at its exit conditions, ALOHA could not model a plume release for CO₂.

Table 5-1: General ALOHA Model Parameters

Parameter	Unit	Value
Atmospheric Temperature	°F	80
Humidity		Dry
Wind Speed	mph	12
Wind Direction		WNW
Population Level		Rural
Terrain		Flat
Cloud Cover	% clear sky	70
Stability Class		D

Professor Ronald Unnerstall, an Assistant Professor teaching Chemical Process Safety at the University of Virginia, was consulted as to how to model the scenario of a pipeline leak with a supercritical fluid. From these discussions, it was determined that accurate results would be

obtained by modeling the CO₂ release as a direct release rather than a pipeline release. The resulting model indicated that the CO₂ concentration would be at safe levels within 10 meters of the release and no graphical model was generated. Even though the health issue is not present for CO₂ releases, the released carbon dioxide is polluted and these amounts would need to be reported to the state of California per state code (California Global Warming Solutions Act of 2006 (AB 32), 2006). Additionally, the ALOHA models were compared to additional ALOHA models from the Sherpa Consulting company in Australia, which works in CO₂ pipeline planning to ascertain validity (Sherpa Consulting Pty Ltd., 2015). ALOHA modeling for CO₂ release was deemed accurate through comparison to the Sherpa charts in terms of chemical composition and plume dispersion over distance in similar weather conditions.

Table 5-2: ALOHA Parameters for Product Pipeline

Parameter	Unit	Value
Pipe Roughness		Smooth
Open End		Connected to Tank
Pipe Diameter	inches	11
Pipe Length	km	3.2 (max)
Pipe Pressure	atm	39.4769
Pipe Temperature	°C	25

Table 5-3: ALOHA Parameters for Input Pipeline

Parameter	Unit	Value
Pipe Roughness		Smooth
Open End		Connected to Tank
Pipe Diameter	cm	40.025
Pipe Length	km	30 (max)
Pipe Pressure	atm	98.6923
Pipe Temperature	°C	25

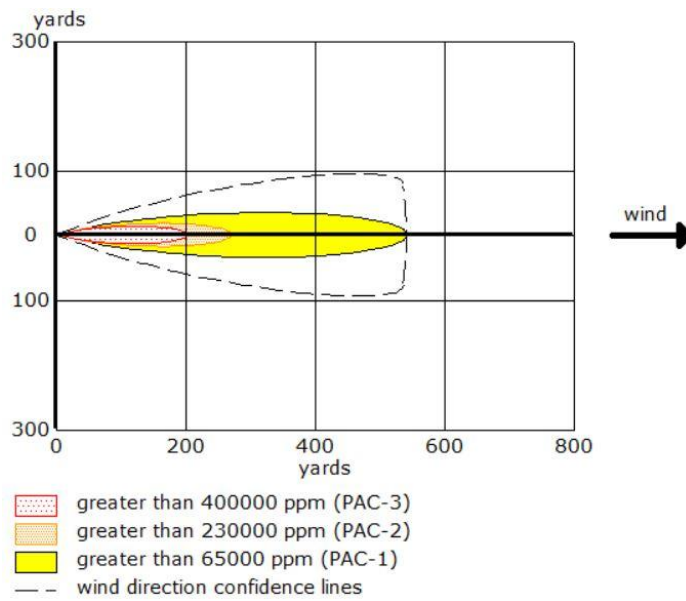


Figure 5-3a: ALOHA Dispersion Model for H₂ Release

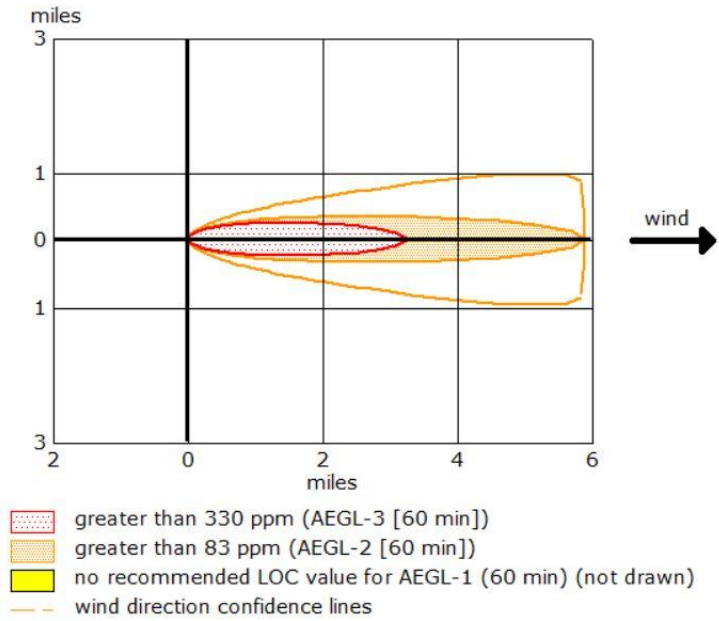


Figure 5-3b: ALOHA Dispersion Model for CO Release

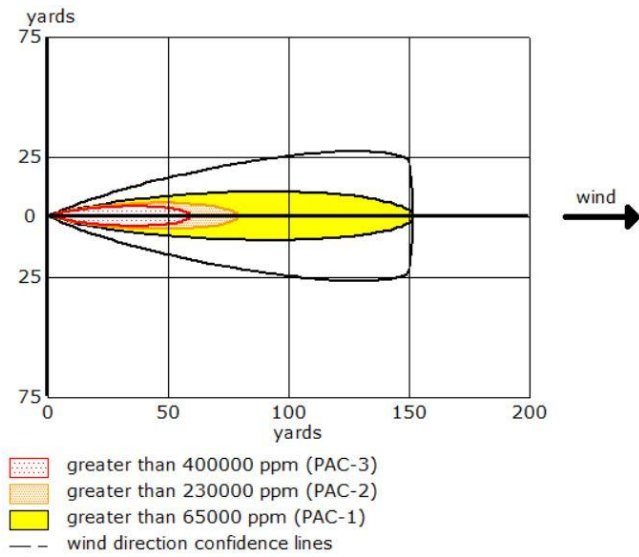


Figure 5-4: ALOHA Dispersion Model for CH₄ Release

5.4 Waste Stream Disposal

The final part of the water separation process is the disposal of the water that is removed from the process, which exits the process at the flash drum. According to Aspen, the water output stream contains no hydrocarbons and a CO₂ concentration of 57 ppm at a previously mentioned 17°C. Had hydrocarbons appeared, a physical adsorption process unit was being considered through the company ECOLOGIX, but this turned out to be unnecessary (ECOLOGIX, 2018). Many regulations are at play to determine what the optimal method of storage or disposal is for this wastewater. While the Clean Water Act does specify that companies must adhere to both federal and state regulations, it does not offer specific marks to be met. The most notable limits are California regulations for hydrocarbon concentration and pH. The California limit of 150 ppm of hydrocarbons (District Code, 2020) is easily met by the proposed process design which emits none and the pH must remain between 6.5-8.5 to be fed into navigable waterways (Water Quality Control Plan, Central Valley Region, Sacramento River and San Joaquin River Basins, 1994). While the team investigated Aspen as a possible manner of determining pH, these efforts were not rewarded with success. The plant process design shows only 0.057 wt% CO₂ in the effluent water stream, which equates to 57 ppm. A large amount of CO₂ might cause acidification, resulting in restricted options for disposal.

A proposed solution to the possible acidification issue the addition of sodium hydroxide (NaOH) to raise the pH Sodium bicarbonate was ruled to not be allowed due to the possible formation of carbonic acid and more CO₂ or CO.

A resource from Utah State University proved useful in correlating the CO₂ concentration in the effluent water stream to an approximate pH, showcased in Figure 5-4 as molarity versus pH (Utah State University, 2021). The process's effluent water stream had a CO₂ mole fraction of 0.0002 which correlates to a pH of 7.5. To be within the California specifications the

concentration of CO₂ must be less than 0.1 mol fraction but more than 0.0001 mole fraction. The proposed process design does not anticipate normal operation to produce CO₂ concentrations outside of these parameters and thus, pH is not an issue for putting effluent water product into an evaporation pond or into nearby waterways.

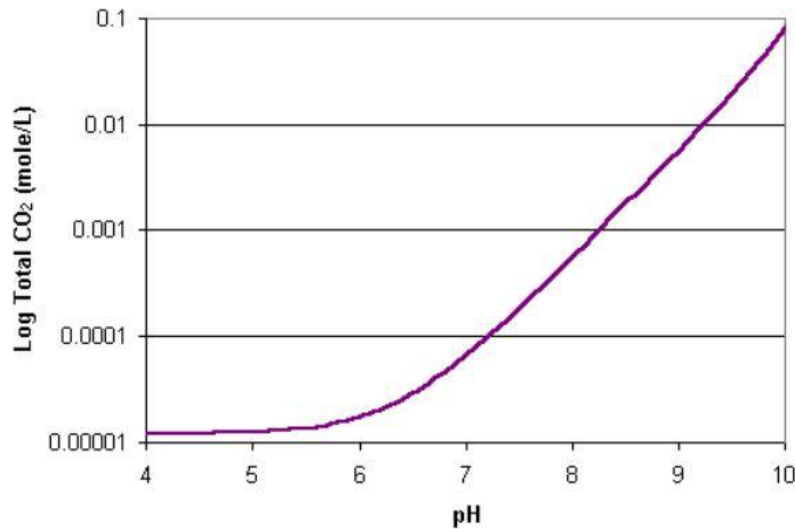


Figure 5-5: CO₂ Concentration versus pH (Utah State University, 2021)

In addition to the liquid water output, the CO₂ outlet stream needs to be kept within certain specifications to be suitable for injection into the wells. The most important specification is that the CO₂ leaves the plant in a supercritical state. Since the plant expels a product stream that is 98.74 wt% CO₂, the temperature-pressure diagram for CO₂ was used as an approximate reference for the state of the product stream. This diagram, as seen in Figure 5-5 was obtained from the University of Saskatchewan in Canada (University of Saskatchewan, 2013). The CO₂ phase diagram clearly shows that carbon dioxide reaches a supercritical fluid state when the temperature is at least 25°C while the pressure is above 100 bar. These standard conditions were kept so that the effluent product stream exited at, or above, the critical point was therefore a supercritical fluid, making transport by pipeline much easier and safer.

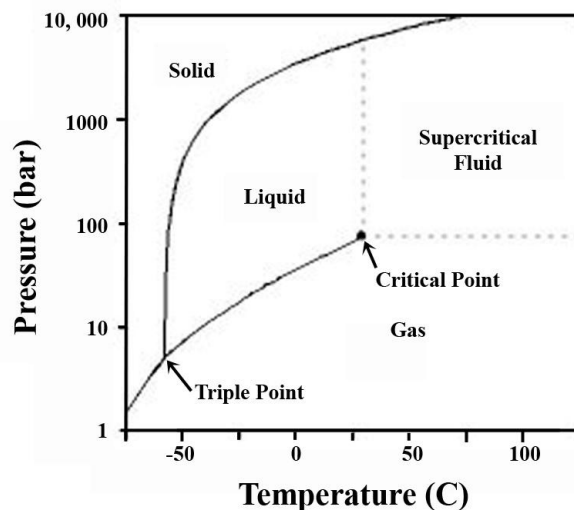


Figure 5-6: Carbon Dioxide Phase Diagram (T vs P) (University of Saskatchewan, 2013)

There are also several composition constraints that also need to be considered for the exit stream to be considered for EOR use. The stream must be dehydrated to less than 1 mol% water while also keeping the CO mol% to less than 5. Beyond these constraints, the oil wells will take anything that has between 90-98 mol% purity of CO₂ (Verma, 2015). The proposed design specifications meet and exceed these requirements set forth by the United States Department of the Interior and are thus well-positioned to be a contending product for drilling companies to purchase for EOR.

5.5 Toxicity

This power plant employs the use of basic hydrocarbons and pure oxygen gas to produce carbon dioxide, water, and a small amount of carbon monoxide as a side product. Due to the simple chemistry involved in the power plant process, there is relatively little toxic danger presented. The most present toxic threat is that of atmospheric oxygen supply displacement. Carbon monoxide is directly toxic if inhaled (Air Gas Inc., 2021b). Hydrogen gas, carbon dioxide, and methane can also displace oxygen in an enclosed environment and lead to rapid suffocation (Air Gas Inc., 2021a; Air Gas Inc., 2021b; Air Gas Inc., 2021c). Additionally, carbon

dioxide can increase heart rate and respiration rate which can trigger or exaggerate other adverse health conditions (Air Gas Inc., 2021a). For a detailed exploration of the safe limits of exposure for these chemicals, see Table 5-4 below.

Table 5-4: Exposure Limits for Common Chemicals

Chemical	OSHA PEL (2016)	
	15 min. (ppm)	8 hrs. (ppm)
Carbon Dioxide	30000	10000
Carbon Monoxide	None listed	50
Hydrogen Gas	None listed	
Methane	None listed	
Oxygen Gas	None listed	

Carbon monoxide has additional toxicology warnings. Rapidly expanding carbon monoxide gas can cause skin or eye burns or frostbite depending on the temperature (Air Gas Inc., 2021b). This same hazard is repeated for hydrogen gas, oxygen gas, and methane.

This project takes place in contained pipelines and unit operations that, in the event of failure, release directly to the atmosphere. With this lack of confined spaces, toxic levels of gas are unlikely to naturally occur. Under normal operation, assuming no deficits, no PPE would be required. However, it is recommended that as a strict safety measure, protective eyewear, thermally insulated industrial work gloves and covered clothing PPE be worn at all times. When conducting maintenance work or in the event of loss of primary containment, respiratory devices and fully protective face shields are required to prevent harm. Carbon monoxide detectors ought to be placed strategically around the facility to ensure proper monitoring of the grounds and a safe working environment. Detectors are even more important since there is not an OSHA PEL (2016) threshold level for 15 minute acute exposure to CO.

Should a toxic level of a chemical release occur, working personnel will be directed to wear proper PPE and remain indoors until the threat has dissipated. To go beyond the standard, an indoor air conditioning system with an uptake away from the facility would improve the safety of indoor spaces in the event of a toxic gas threat, but might be too expensive to be employed.

6. Conclusions and Recommendations

6.1 Financial Considerations

Based on the current financial estimations presented in Section 4.4.4, the plant design will lose \$4.12 million annually when at full operational capacity. Therefore, it is encouraged that this plant design does not move onto the next stage of development without additional changes. Further design will potentially uncover more expenses for equipment and construction as shown with the FCI range, \$180 million to \$393 million, mostly including costs higher than the predicted FCI of \$265 million. Because further design will also likely not increase the output of CO₂ or electricity significantly, the plant design will most likely not become financially viable under the current economic conditions.

As discussed in Section 4.4.4, if the current economic conditions changed favorably such that the price of products increased or the cost of raw materials decreased, this design could be financially sustainable. The largest income to the plant would be from the electricity sales, so an increase in the wholesale price of electricity from \$46.45 / MWh to \$47.78 / MWh would be the most feasible way for the plant to become profitable. Although \$46.45 / MWh was the highest average wholesale price for all major electricity hubs in the U.S. in 2020, the prices fluctuated significantly with a highest daily average price of \$1639.60 / MWh, showing that the increase is reasonable (*Wholesale Electricity and Natural Gas Market Data*, 2021). Additionally, lowering the cost of oxygen from \$0.07 / kg to \$0.067 / kg would make the plant profitable. Incorporating the ASU into the process design would also decrease the cost of raw materials as the financials would no longer account for paying the vendor such as Air Liquide to supply the oxygen to the process. Under either of these different economic scenarios or a combination of them both the plant design would be financially viable.

6.2 Recommendations and Future Work

A potential path to future process efficiency improvements lies in heat integration. To achieve maximum efficiency, Allam stipulates that there must be a small temperature difference at the hot end of the recuperator. A large difference in specific heat between the recycle stream and the turbine exhaust stream necessitates an additional source of heat in the range of 100°C to 400°C in order to achieve this temperature approach (R. Allam et al., 2017).

To accomplish this small temperature difference, the first option would be to integrate heat liberated from the dry CO₂ exhaust during recompression in C-102 into a series of recuperating heat exchangers. The simulation could be modified so that the dry CO₂ stream out of stage 1 of the compressor is first passed through an additional recuperator before passing through the first intercooler such that the duty of the intercooler is lowered and a small amount of heat is transferred into the CO₂ and oxidant recycle streams. Depending on the quality of the heat from each compression stage, both streams leaving the compression stages could be integrated in this manner. A preliminary design which integrates one of the compressed streams into heat recuperation can be seen in figure 6-1.

This layout allows for a small amount of heat to be transferred such that a closer temperature approach at the hot end of the heat exchanger is achieved. It was found to be extremely difficult to integrate this heat due to its low quality and the occurrence of temperature crossovers. Furthermore, a more complex arrangement of recuperating heat exchangers was required to avoid temperature crossovers - the first stage compressed CO₂ stream was used to heat the recycle streams in between partial heating from the turbine exhaust. Integration of this heat only allowed for a slight increase in net electricity generation of around 20 MW. While this

may be considered as a first step towards efficient heat integration, future work would be necessary to optimize this layout such that process efficiency is maximized.

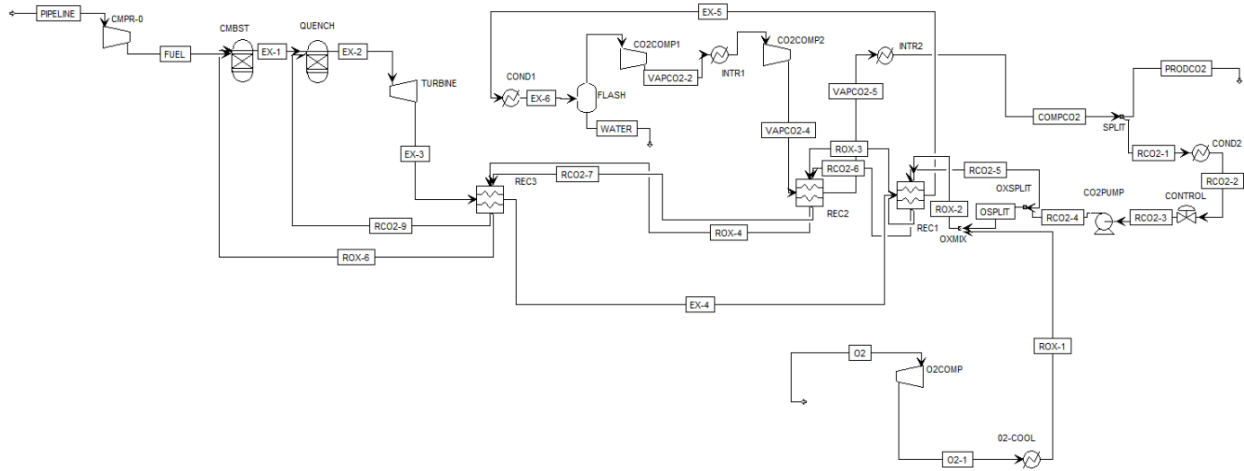


Figure 6-1: Modified Allam Cycle PFD with CO₂ Compressor Heat Integration

Another option for heat integration, which is included in the original cycle design by Allam, is to integrate heat from an on-site ASU. Heat liberated from air during cryogenic air separation can serve as a convenient form of heat that can be integrated to achieve a close temperature approach in the hot end of the recuperator (R. Allam et al., 2017). This heat could be integrated in a similar manner as was attempted for heat from the CO₂ compressor. While utilizing an onsite air separation unit leads to an energy penalty of approximately 12% of gross electrical output from the turbine, the ability to produce oxygen at a lower price, the ability to sell value added nitrogen and argon, and more efficient heat integration in combination would be expected to yield greater profitability (Goff, 2019). Not factoring in the benefit of ASU heat integration, the net difference between the capital saved and earned against the revenue lost can be estimated to determine if these changes make the design financially feasible.

Argon gas can be sold at \$30/ton and nitrogen gas can be sold at \$8/ton (Goff, 2019). Due to the composition of atmospheric air, approximately 78 moles of nitrogen and 0.9 moles of argon can be extracted for every 21 moles of oxygen extracted for the process. As the current design of the process requires 2.5 kmol/s of oxygen, it is expected that an on-site ASU could feasibly produce 9.29 kmol/s of nitrogen and 0.11 kmol/s of Argon from feed air that is of no cost. Including contributions from the assumed capacity factor, this would equate to product streams that can be sold for approximately \$37,600,000 in nitrogen per year and \$2,400,000 in argon per year. Because oxygen would be derived from air, its only cost is 12% of gross energy from the turbine such that raw material costs become approximately \$102,000,000 less and revenue from sold electricity is reduced by \$17,300,000. Overall, this would result in a gain in I/O profit of approximately \$124,700,000, which would likely be enough to make the plant profitable. There are other costs associated with running an ASU, however, such as additional operators and a reduction in profit from taxes, and not enough is currently known about the energy penalty of running an ASU at large scales. An ASU is also a complex piece of technology that would be extremely expensive to design, purchase, and install such that capital costs would be sacrificed for greater profitability. Because integration of an ASU is expected to make the project profitable, this is a recommended path for future Allam cycle research.

7. Acknowledgements

Many thanks are given to Professor Eric W. Anderson for his knowledge, guidance, and assistance throughout the duration of the project.

Thanks are in order to Professor Ronald Unnerstall for his contributions to the safety and hazard sections of the process and for his guidance in using the ALOHA and MARPLOT software to determine safe operating conditions and locations.

Thanks are given to Professor William Epling, chair of the Department of Chemical Engineering in the School of Engineering and Applied Science at the University of Virginia for his knowledge and guidance to the team in reference to the Allam cycle, Allam papers, and the pilot plants already in existence.

8. Table of Nomenclature

Table 8-1. Acronyms and shorthands	
RET	Renewable Energy Technology
CCS	Carbon Capture and Sequestration
MWe	Electricity input or output in MW
MWth	Thermal energy input in MW
ASU	Air Separation Unit
LOX	Liquid Oxygen
EOR	Enhanced Oil Recovery
EIA	U.S. Energy Information Administration
NGCC	Natural Gas Combined Cycle
NO _x	Nitrous Oxides
RGIBBS	Gibbs Reactor Model
LMTD	Logarithmic Mean Temperature Difference
EPA	U.S. Environmental Protection Agency
ALOHA	Areal Locations of Hazardous Atmospheres
CAMEO	Computer-Aided Management of Emergency Operations
PPE	Personal Protective Equipment
LOPC	Loss of Primary Containment
SCC	Stress Corrosion Cracking
MOC	Materials of construction
SO _x	Sulfur Oxides
FCI	Fixed Capital Investment

Table 8-2. Variables	
V_G	Maximum allowable gas velocity in drum (m/s)
ρ_L	Liquid density (kg/m ³)
ρ_V	Vapor density (kg/m ³)
k_E	Deentrainer constant
r_o	Tube outer radius (m)
r_i	Tube inner radius (m)
U_o	Overall heat transfer coefficient (W/m ² K)
h	Convective heat transfer coefficient (W/m ² K)
k	Thermal conductivity (W/mK)
Nu	Nusselt number
Re	Reynolds number
Pr	Prandtl number
d_o	Outer diameter (m)
ΔT_{lm}	Logarithmic mean temperature difference (K)
T_i	Hot stream temperature on side i (K)
t_i	Cold stream temperature on side i (K)
ΔT_i	Temperature difference on side i (K)
Q_H	Hot stream heat duty (W)
A_o	Heat transfer area (m ²)
F	LMTD Correction factor
l_T	Tube length (m)
N_{tubes}	Number of tubes
T_{DB}	Dry bulb temperature (°C)
T_{WB}	Wet bulb temperature (°C)

Table 8-2. Variables (cont.d)	
$Rh\%$	Relative humidity (%)
A_c	Cross sectional area (m ²)
V_D	Drum volume (m ³)
H_D	Drum height (m)
b	Plate spacing (m)
\dot{m}	Mass flow rate (kg/s)
W	Plate width (m)
NP	Number of plates
μ	Viscosity (Pa-s)
U	Overall heat transfer coefficient, plate heat exchanger (W/m ² K)
Re	Reynolds number
Pr	Prandtl number
V_R	Reactor volume (m ³)
v_0	Inlet volumetric flow rate (m ³ /s)
τ	Reactor residence time (s)
\dot{n}_i	Molar flow rate (kmol/s)
\dot{W}_{net}	Net work of process (MW)
$\eta_{overall}$	Overall efficiency of process
\dot{q}_{loss}	Heat loss from process (MW)
α	Fractional excess of methane
\hat{H}_i	Enthalpy of stream i (kJ/mol)
C_{OL}	Operating Labor Cost
C_{WT}	Waste Treatment Cost
C_{RM}	Raw Materials Cost

Table 8-2. Variables (cont.d)	
C_{UT}	Utility Cost
C_{OM}	Cost of Manufacturing

9. References

AICHE. (2014, December 18). *CCPS Process Safety Glossary* | AICHE.

<https://www.aische.org/ccps/resources/glossary>

Air Gas Inc. (2021a). *Carbon Dioxide—SDS No. 001013*.

Air Gas Inc. (2021b). *Carbon Monoxide—SDS No. 001014*.

AirGas Inc. (2021a). *Hydrogen Gas—SDS No. 001026*.

AirGas Inc. (2021b). *Methane—SDS No. 001033*.

Allam, R. J., Palmer, M. R., Brown, G. W., Fetvedt, J., Freed, D., Nomoto, H., Itoh, M., Okita, N., & Jones, C. (2013). High Efficiency and Low Cost of Electricity Generation from Fossil Fuels While Eliminating Atmospheric Emissions, Including Carbon Dioxide. *Energy Procedia*, 37, 1135–1149. <https://doi.org/10.1016/j.egypro.2013.05.211>

Allam, R., Martin, S., Forrest, B., Fetvedt, J., Lu, X., Freed, D., Brown, G. W., Sasaki, T., Itoh, M., & Manning, J. (2017). Demonstration of the Allam Cycle: An update on the development status of a high efficiency supercritical carbon dioxide power process employing full carbon capture. *Energy Procedia*, 114, 5948–5966. <https://doi.org/10.1016/j.egypro.2017.03.1731>

ArcGis. (2021). *Gas Transmission Pipeline Interactive Map—Kern*.

<https://socialgas.maps.arcgis.com/apps/webappviewer/index.html?id=09d70253280b4792b7a6a3fa6a2cf4a7>

Blau, M. (2020, January 15). *“I’ve quit drinking the water”*: What it’s like to live next to America’s largest coal plant | Grist.

<https://grist.org/energy/ive-quit-drinking-the-water-what-its-like-to-live-next-to-americas-largest-coal-plant/>

Bureau of Labor Statistics. (2021a). *Employer Costs for Employee Compensation—December 2020*. 12.

Bureau of Labor Statistics. (2021b, March 31). *Chemical Plant and System Operators*.

<https://www.bls.gov/oes/current/oes518091.htm>

California Global Warming Solutions Act of 2006 (AB 32), (2006).

California ISO - Today's Outlook. (2021, April 14).

<http://www.caiso.com/TodaysOutlook/Pages/index.html>

California Weather Data: Formatted report—UC IPM. (n.d.). Retrieved March 15, 2021, from

<http://ipm.ucanr.edu/calludt.cgi/WXDATAREPORT#summary>

Cooling Tower Efficiency. (n.d.). Retrieved March 27, 2021, from

https://www.engineeringtoolbox.com/cooling-tower-efficiency-d_699.html

Couper, J. R., Penney, W. R., Fair, J. R., & Walas, S. M. (Eds.). (2010). 18—PROCESS

VESSELS. In *Chemical Process Equipment (Revised Second Edition)* (pp. 641–661).

Gulf Professional Publishing. <https://doi.org/10.1016/B978-0-12-372506-6.00015-0>

Crane, R. (2020). *2019 Outlook for Energy: A Perspective to 2040*.

District Code. (2020, November 17). *Chapter 5.20 WASTEWATER DISCHARGE AND PRETREATMENT REGULATIONS*.

<https://www.codepublishing.com/CA/DublinSRSD/html/DublinSRSD05/DublinSRSD0520.html#5.20.050>

ECOLOGIX. (2018). *Hydrocarbon Removal Oil Water Separation Products » Ecologix Systems*.

<https://www.ecologixsystems.com/product-ows-oilfree/>

EIA. (n.d.). *Electric Power Monthly—U.S. Energy Information Administration (EIA)*. Retrieved

April 14, 2021, from https://www.eia.gov/electricity/monthly/epm_table_grapher.php

- EIGA. (2004). *Carbon Monoxide and Syngas Pipeline Systems* (Globally Harmonized Document 120/04/E). European Industrial Gas Association.
- Goff, A. (2019, April). *NET Power*.
https://www.cslforum.org/cslf/sites/default/files/documents/Champaign2019/Update-on-NET-Power-Project_TG-Meeting-April-2019.pdf
- Goodyear, S. (2013, August 15). *For Some in the Southwest, It's Come to Selling Water to Fracking Companies*.
<https://nextcity.org/daily/entry/for-some-in-the-southwest-its-come-to-selling-water-to-fracking-companies>
- Government of Canada, C. C. for O. H. and S. (2021, March 30). *Methane: OSH Answers*.
<https://www.ccohs.ca/>
- Liu, Y., Wang, Y., & Huang, D. (2019). Supercritical CO₂ Brayton cycle: A state-of-the-art review. *Energy*, 189, 115900. <https://doi.org/10.1016/j.energy.2019.115900>
- Middleman, S. (1997). *An Introduction to Mass and Heat Transfer: Principles of Analysis and Design* (1st edition). Wiley.
- NaturalGas.org. (2013, September 20). » *The Transportation of Natural Gas* *NaturalGas.org*.
<http://naturalgas.org/naturalgas/transport/>
- Olson, D. A. (2000). *Heat transfer of supercritical carbon dioxide flowing in a cooled horizontal tube* (NIST IR 6496; p. NIST IR 6496). National Institute of Standards and Technology.
<https://doi.org/10.6028/NIST.IR.6496>
- Patel, S. (2019, November 27). 300-MW Natural Gas Allam Cycle Power Plant Targeted for 2022. *POWER Magazine*.
<https://www.powermag.com/300-mw-natural-gas-allam-cycle-power-plant-targeted-for-2022/>

Peletiri, S. P., Rahmanian, N., & Mujtaba, I. M. (2018). CO2 Pipeline Design: A Review.

Energies, 11(2184). <https://doi.org/10.3390>

Peters, M., Timmerhaus, K., West, R., & Peters, M. (2002). *Plant Design and Economics for Chemical Engineers* (5th edition). McGraw-Hill Education.

Power blocks in natural gas-fired combined-cycle plants are getting bigger—Today in

Energy—U.S. Energy Information Administration (EIA). (n.d.). Retrieved March 28,

2021, from <https://www.eia.gov/todayinenergy/detail.php?id=38312>

PubChem. (n.d.). *Methane*. Retrieved April 14, 2021, from

<https://pubchem.ncbi.nlm.nih.gov/compound/297>

Sherpa Consulting Pty Ltd. (2015). *Dispersion Modeling Techniques for Carbon Dioxide*

Pipelines in Australia.

Short-Term Energy Outlook—U.S. Energy Information Administration (EIA). (n.d.). Retrieved

March 28, 2021, from <https://www.eia.gov/outlooks/steo/report/electricity.php>

Turton, R., Shaeiwitz, J., Bhattacharyya, D., & Whiting, W. (2018). *Analysis, Synthesis, and*

Design of Chemical Processes, Fifth Edition. Prentice Hall.

<https://proquest.safaribooksonline.com/9780134177502>

University of Saskatchewan. (2013, June 9). *CDP instruction*.

<http://www.usask.ca/biology/scopes/CDP%20instruction.html>

Unnerstall, R. (2021). *Pre-read- Laboratory Safety October 6th, October 8th*.

US EPA, O. (2013, August 1). *CAMEO (Computer-Aided Management of Emergency*

Operations) [Collections and Lists]. US EPA. <https://www.epa.gov/cameo>

Water quality control plan, Central Valley Region, Sacramento River and San Joaquin River

Basins, III (1994).

Utah State University. (2021). *Dissolved carbon dioxide*.

<http://ion.chem.usu.edu/~sbialkow/Classes/3650/CO2%20Solubility/DissolvedCO2.html>

Verma, M. K. (2015). *Fundamentals of carbon dioxide-enhanced oil recovery (CO₂-EOR)—A supporting document of the assessment methodology for hydrocarbon recovery using CO₂-EOR associated with carbon sequestration*. U.S. Geological Survey.

Weather Spark. (n.d.). *Average Weather in Bakersfield, California, United States, Year Round—Weather Spark*. Retrieved March 30, 2021, from

<https://weatherspark.com/y/1451/Average-Weather-in-Bakersfield-California-United-States-Year-Round>

Wet Bulb Calculator. (n.d.). Omni Calculator. Retrieved March 15, 2021, from

<https://www.omnicalculator.com/physics/wet-bulb>

Wet Bulb Temperatures and Cooling Tower Performance | Delta Cooling Towers, Inc. (2017, April 27). Manufacturers of Cooling Towers & Systems by Delta Cooling Towers, Inc.

<https://deltacooling.com/resources/news/understanding-wet-bulb-temperatures-and-how-it-affects-cooling-tower-performance>

Wholesale electricity and natural gas market data. (2021, April 8). U.S. Energy Information

Administration. <https://www.eia.gov/electricity/wholesale/#history>

Zhang, X., Keramati, H., Arie, M., Singer, F., Tiwari, R., Shooshtari, A., & Ohadi, M. (2018).

Recent developments in high temperature heat exchangers: A review. *Frontiers in Heat and Mass Transfer*, 11. <https://doi.org/10.5098/hmt.11.18>

10. Appendix

10.1 Equations

$$A = \frac{Q_H}{U^* \Delta T_{lm}} \quad (3-1)$$

$$\Delta T_{lm} = \frac{\Delta T_1 - \Delta T_2}{\ln(\Delta T_1 / \Delta T_2)} \quad (3-2)$$

$$\frac{1}{U} = \frac{1}{h_{cold\ stream}} + \frac{1}{h_{hot\ stream}} \quad (3-3)$$

$$h = \frac{kNu}{2bF} = \frac{k(0.0296Re^{0.8}Pr^{0.33})}{2bF} \quad (3-4)$$

$$Re = \frac{4 \dot{m}}{W(NP-1)\mu} \quad (3-5)$$

$$V_G = k_E(\rho_L/\rho_V - 1)^{1/2} \quad (3-6)$$

$$\frac{1}{U_0} = \frac{1}{h_0} + \frac{r_0}{k} \ln\left(\frac{r_0}{r_i}\right) + \frac{1}{h_i} \frac{r_0}{r_i} \Rightarrow \frac{1}{U_0} = \frac{1}{h_0} \quad (3-7)$$

h_0 and h_i represent the convective heat transfer coefficients on the shell side and tube side, respectively. k represents the thermal conductivity of the tubes.

$$Nu = \frac{hd_0}{k} \quad (3-8)$$

h and k refer to the heat transfer properties of the supercritical CO₂ stream according to the Aspen model.

$$S = \frac{t_2 - t_1}{T_1 - t_1} \quad (3-9)$$

$$R = \frac{T_1 - T_2}{t_2 - t_1}$$

S and R are dimensionless quantities used in conjunction with Figure 3-1 for determination of the LMTD correction factor. The hot and cold streams for the case of the condenser are the shell side CO₂ and the tube side cooling water, respectively.

$$Q_H = U_0 A_0 F \Delta T_{lm} \quad (3-10)$$

$$A_0 = 2\pi r_0 l^* N_{tubes} \quad (3-11)$$

$$T_{WB} = T_{DB} * \arctan[0.151977(Rh\% + 8.313659)^{1/2}] \quad (3-12)$$

$$+ \arctan(T_{DB} + Rh\%) - \arctan(Rh\% - 1.676331)$$

$$+ 0.00391838Rh\%^{3/2} * \arctan(0.023101Rh\%) - 4.686035$$

$$\tau = \frac{V_R}{v_o} \quad (3-13)$$

$$\dot{w}_{net} - \dot{q}_{loss} = \frac{\dot{w}_{net}}{\eta_{overall}} = (\dot{n}\hat{H})_{CH_4} + (\dot{n}\hat{H})_{Air} - (\dot{n}\hat{H})_{CO_2} - (\dot{n}\hat{H})_{CH_4,out} - (\dot{n}\hat{H})_{H_2O} - (\dot{n}\hat{H})_{N_2} \quad (3-14)$$

$$\dot{n}_{Air} = \frac{2\dot{n}_{CH_4}}{0.21(1 + \alpha)} \quad (3-15)$$

$$\dot{n}_{CO_2} = \frac{\dot{n}_{CH_4}}{(1 + \alpha)} \quad (3-16)$$

$$\dot{n}_{CH_4,out} = \frac{\alpha\dot{n}_{CH_4}}{(1 + \alpha)} \quad (3-17)$$

$$\dot{n}_{N_2} = \frac{2(0.79)\dot{n}_{CH_4}}{(0.21)(1 + \alpha)} \quad (3-18)$$

$$\dot{n}_{H_2O} = \frac{2\dot{n}_{CH_4}}{(1 + \alpha)} \quad (3-19)$$

$$\frac{\dot{w}_{net}}{\eta_{overall}} = \dot{n}_{CH_4} \left[\hat{H}_{CH_4} + \frac{2\hat{H}_{Air}}{0.21(1+\alpha)} - \left(\frac{1}{(1+\alpha)} \right) (\hat{H}_{CO_2} + \alpha\hat{H}_{CH_4,out} + 2\hat{H}_{H_2O} + \frac{2(0.79)\hat{H}_{N_2}}{(0.21)}) \right] \quad (3-20)$$

$$N_{OL} = (6.29 + 31.7P^2 + 0.23N_{np})^{0.5} \quad (4-1)$$

$$C_{OM} = 0.280FCI = 2.73C_{OL} + 1.23(C_{UT} + C_{WT} + C_{RM}) \quad (4-2)$$

10.2 Sample Calculations

Recuperator area:

The convective heat transfer coefficient for stream RCO2-4 is shown using Equations 3-4 and 3-5.

$$Re = \frac{4 \text{ in}}{W(NP-1)\mu} = \frac{4*947.332}{1*(217-1)*7.00*10^{-5}} = 2.51 * 10^5$$

$$h = \frac{k(0.0296Re^{0.8}Pr^{0.33})}{2bF} = \frac{0.0167*(0.0296*(2.51*10^5)^{0.8}(7.309)^{0.33})}{2*0.003*1} = 4185.58 \text{ W/m}^2\text{K}$$

The overall heat transfer coefficient and LMTD between streams RCO2-4 and EX-3 are shown using Equations 3-2 and 3-3.

$$\frac{1}{U} = \frac{1}{h_{\text{cold stream}}} + \frac{1}{h_{\text{hot stream}}} = \frac{1}{4185.58} + \frac{1}{1417.61} \Rightarrow U = 1058.95 \text{ W/m}^2\text{K}$$

$$\Delta T_{lm} = \frac{\Delta T_1 - \Delta T_2}{\ln(\Delta T_1 / \Delta T_2)} = \frac{(803.08 - 717) - (79.24 - 62.88)}{\ln((803.08 - 717) / (79.24 - 62.88))} = 41.99 \text{ K}$$

Finally for area needed between streams RCO2-4 and EX-3 is shown using Equations 3-1 and the final area for the recuperator is summed.

$$A = \frac{887.49*10^6}{1058.95*41.99} = 2660.66 \text{ m}$$

$$A_{\text{Total}} = \sum A = 2660.66 + 1213.65 = 3874.31 \text{ m}$$

Flash drum sizing:

Sizing the flash drum of the water separation unit is shown below. To begin, the maximum gas velocity is estimated using equation 3-6. k_E was chosen to be 0.1 for the presence of a mesh deentrainer.

$$V_G = k_E (\rho_L / \rho_V - 1)^{1/2} = 0.1 * \left(\frac{1002 \text{ kg/m}^3}{67.6 \text{ kg/m}^3} - 1 \right)^{1/2} = 0.372 \text{ m/s}$$

The volumetric flow rate of gas is then divided by the gas velocity to determine cross sectional area.

$$A_c = 20.9 \text{ m}^3 / 0.372 \text{ m/s} = 56.1 \text{ m}^2$$

The diameter is then calculated using the area of a circle as follows and the length of the drum is calculated using the assumed L/D ratio.

$$D = \left(\frac{4A_c}{\pi} \right)^{1/2} = \left(\frac{4 * 56.1 \text{ m}^2}{3.14} \right)^{1/2} = 8.45 \text{ m}$$

$$H = 2.5 * D = 2.5 * 8.45 \text{ m} = 21.1 \text{ m}$$

Finally, the volume of the drum is calculated by multiplying the cross sectional area of the drum by the drum height.

$$V_D = A_c * H_D = 56.1 \text{ m}^2 * 21.1 \text{ m} = 1186 \text{ m}^3$$

Condenser Sizing

Sizing the condenser before the flash drum is simple but calculation intensive as seen below.

First, the LMTD is calculated using equation 3-2.

$$\Delta T_{lm} = \frac{\Delta T_1 - \Delta T_2}{\ln(\Delta T_1 / \Delta T_2)} = \frac{(17^\circ\text{C} - 13.3^\circ\text{C}) - (79^\circ\text{C} - 21.6^\circ\text{C})}{\ln\left(\frac{17^\circ\text{C} - 13.3^\circ\text{C}}{79^\circ\text{C} - 21.6^\circ\text{C}}\right)} = 19.6 \text{ K}$$

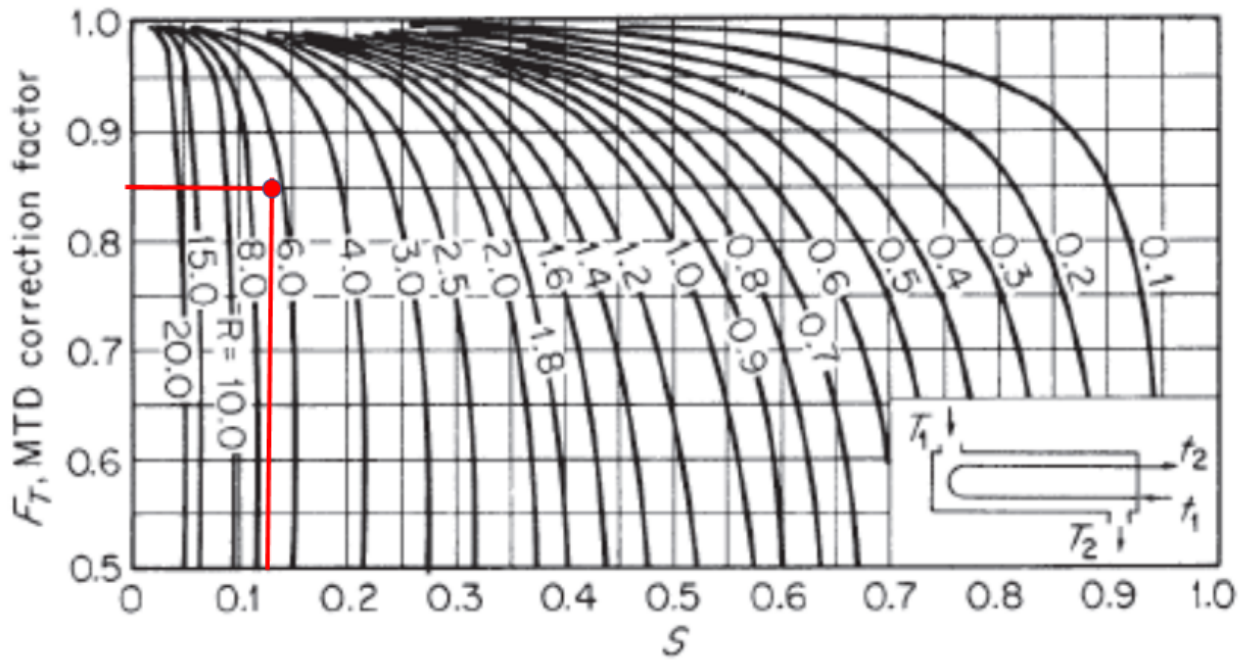
Next, a convective heat transfer coefficient for CO₂ is calculated using an assumed Nusselt number, and that value is taken as the overall heat transfer coefficient (eqns. 3-7 and 3-8).

$$U_0 = h = \frac{Nu * k}{d_o} = \frac{1791.5 * 0.0184 \text{ W/mK}}{0.0192 \text{ m}} = 1730 \text{ W/m}^2\text{K}$$

S and R are calculated using equation 3-9 and the corresponding LMTD correction factor F is pulled from Figure 10-1 using graphical interpolation.

$$S = \frac{t_2 - t_1}{T_1 - t_1} = \frac{21.3^\circ\text{C} - 13.3^\circ\text{C}}{79^\circ\text{C} - 13.3^\circ\text{C}} = 0.13$$

$$R = \frac{T_1 - T_2}{t_2 - t_1} = \frac{79^\circ\text{C} - 17^\circ\text{C}}{21.6^\circ\text{C} - 13.3^\circ\text{C}} = 7.5$$



$$F = 0.85$$

Next, a total heat transfer area is calculated using equation 3-10. The number of tubes required for this heat transfer area is calculated with equation 3-11.

$$A_0 = \frac{Q_H}{U_0 F \Delta T_{lm}} = \frac{1.28 \times 10^8 \text{ W}}{1730 \text{ W/m}^2\text{K} * 0.85 * 19.6^\circ\text{C/K}} = 4446 \text{ m}^2$$

$$N_{tubes} = \frac{A_0}{2\pi r_0 l} = \frac{4446 \text{ m}^2}{2 * 3.14 * 0.0095 \text{ m} * 15 \text{ m}} = 4953$$

This procedure was also followed to size the intercoolers in the CO₂ compressor, C-102.

Combustor Sizing

Sizing the combustor required the use of equation 3-13. It was relatively simple once CHEMKED-II had been used to gather the residence time as the aspen model already knew the volumetric input to the combustion chamber.

$$\tau = \frac{V_R}{v_o}$$
$$\tau \cdot v_o = V_R$$

Given that the residence time is 0.26 s and the volumetric input is 6.82 m³/s V_R can be found.

$$0.26 (s) \cdot 6.82 m^3/s = 1.77 m^3$$

10.3 Computer Software

10.3.1 AspenPlus v11

AspenPlus v11 is a professional modeling software that was used with permission of the owner AspenTech through a licensed partnership with the University of Virginia. The software created process flow diagrams, simulated the process to give material and energy balances, informed basic utility appraisals, and generated data for thermodynamic and kinetic evaluation (such as sizing of unit operations and physical state of streams in the process).

10.3.2 CHEMKED II

CHEMKED II is a modeling software package, developed at MIT that simulates complicated combustion processes. The GRIMech 30 methane combustion package was used in this project to determine equilibrium data for methane combustion and to discover the residence time of the reaction, a necessary component required for the sizing of the combustor.

10.3.3 Microsoft Excel

Microsoft Excel (Excel) is a spreadsheet analysis software that is available as part of the Microsoft Office Suite license through the Microsoft Corporation. Excel formatted data for tables

and performed balancing calculations outside of AspenPlus for balances and dispersion modeling.

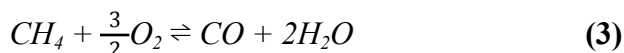
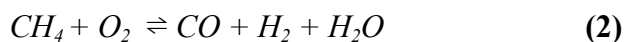
10.3.4 ALOHA/CAMEO/MARPLOT

The CAMEO (Computer-Aided Management of Emergency Operations) suite is a software program made available by the Environmental Protection Agency (EPA) and National Oceanic and Atmospheric Association (NOAA) to assist in modeling chemical releases. CAMEO specifically stores chemical data on commonly known, studied, and used substances in industry. ALOHA (Areal Locations of Hazardous Atmospheres) combined CAMEO's data with weather conditions and the conditions of the release to produce the release dispersion models. MARPLOT can plot ALOHA's models onto digital maps, but this was not used in this project.

10.3.5 CRW

AICHE's Chemical Reactivity Worksheet software provides information about thousands of common hazardous chemicals. This data is used to inform material of construction decisions as well as potential storage and handling hazards. Groups that have collaborated to develop CRW are: Center for Chemical Process Safety, Environmental Protection Agency, NOAA's Office of Response and Restoration, The Materials Technology Institute, Dow Chemical Company, Dupont, Phillips.

10.4 Primary Reactions



10.5 Equipment Capital Costs

Table 10-1: Plant and Equipment Capital Costs on CAPCOST

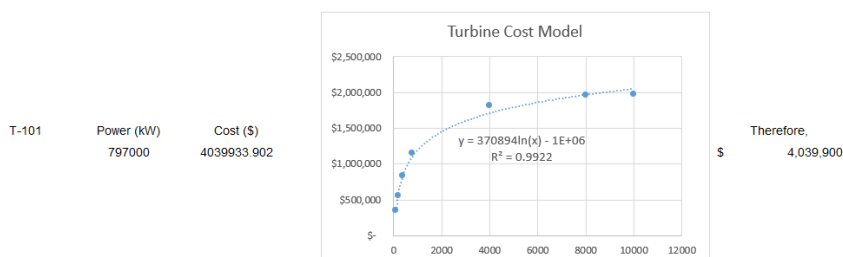
Compressors	Compressor Type	Power (kilowatts)	# Spares	MOC	Purchased Equipment Cost	Bare Module Cost	Base Equipment Cost	Base Bare Module Cost
C-101	Centrifugal	8067	1	Carbon Steel	\$ 4,720,000	\$ 12,900,000	\$ 4,720,000	\$ 12,900,000
C-102-1	Centrifugal	40401	0	Carbon Steel	\$ 11,500,000	\$ 31,600,000	\$ 11,500,000	\$ 31,600,000
C-103	Centrifugal	8411	1	Carbon Steel	\$ 4,850,000	\$ 13,300,000	\$ 4,850,000	\$ 13,300,000
C-102-2	Centrifugal	32400	0	Carbon Steel	\$ 9,180,000	\$ 25,200,000	\$ 9,180,000	\$ 25,200,000

Exchangers	Exchanger Type	Shell Pressure (barg)	Tube Pressure (barg)	MOC	Area (square meters)	Purchased Equipment Cost	Bare Module Cost	Base Equipment Cost	Base Bare Module Cost
E-101	Flat Plate		330	Nickel	969	\$ 1,440,000	\$ 2,260,000	\$ 537,000	\$ 1,160,000
	Flat Plate		330	Stainless Steel	2910	\$ 1,310,000	\$ 6,320,000	\$ 1,610,000	\$ 1,160,000
E-102	Floating Head	29	0	Carbon Steel / Carbon Steel	4450	\$ 978,000	\$ 3,050,000	\$ 874,000	\$ 2,870,000
C-102 Intercoolers	Floating Head	53.8	0	Carbon Steel / Carbon Steel	2620	\$ 632,000	\$ 1,890,000	\$ 515,000	\$ 1,690,000
	Floating Head	99	0	Carbon Steel / Carbon Steel	6850	\$ 1,870,000	\$ 5,300,000	\$ 1,350,000	\$ 4,450,000

Pump	Type	Power (kilowatts)	# Spares	MOC	Discharge Pressure (barg)	Purchased Equipment Cost	Bare Module Cost	Base Equipment Cost	Base Bare Module Cost
P-101	Centrifugal	64500	1	Carbon Steel	330	\$ 313,000	\$ 124,200,000	\$ 17,700,000	\$ 267,000

Reactors	Type	Volume (cubic meters)	Purchased Equipment Cost	Bare Module Cost	Base Equipment Cost	Base Bare Module Cost
R-101	Autoclave	2.99	\$ 60,600	\$ 242,000	\$ 60,600	\$ 242,000

Turbines	Turbine Type	Power (kilowatts)	# Spares	MOC	Purchased Equipment Cost	Bare Module Cost	Base Equipment Cost	Base Bare Module Cost
J-101	Axial	797	0	Nickel Alloy	\$ 1,150,000	\$ 4,010,000	\$ 344,000	\$ 1,200,000
J-102	Axial	400	0	Nickel Alloy	\$ 834,000	\$ 2,920,000	\$ 250,000	\$ 876,000
J-103	Axial	200	0	Nickel Alloy	\$ 562,000	\$ 1,970,000	\$ 169,000	\$ 591,000
J-104	Axial	100	0	Nickel Alloy	\$ 352,000	\$ 1,230,000	\$ 106,000	\$ 370,000
J-105	Axial	10000	0	Nickel Alloy	\$ 1,970,000	\$ 6,900,000	\$ 592,000	\$ 2,070,000
J-106	Axial	4000	0	Nickel Alloy	\$ 1,820,000	\$ 6,350,000	\$ 545,000	\$ 1,910,000
J-107	Axial	8000	0	Nickel Alloy	\$ 1,960,000	\$ 6,840,000	\$ 587,000	\$ 2,050,000



Vessels	Orientation	Length/Height (meters)	Diameter (meters)	MOC	Demister MOC	Pressure (barg)	Purchased Equipment Cost	Bare Module Cost	Base Equipment Cost	Base Bare Module Cost
V-101	Vertical	21.8	8.72	Carbon Steel	Stainless Steel	30	\$ 17,000,000	\$ 33,400,000	\$ 1,250,000	\$ 4,720,000
Totals							\$ 57,893,500	\$ 289,882,000	\$ 56,739,600	\$ 108,626,000

Total Module Cost \$ 342,060,000
Total Grass Roots Cost \$ 396,370,000
Total Equipment Cost \$ 57,893,500

Lang Factor 4.74
Lang Factor Cost \$ 274,400,000
 High Range, 148% \$ 406,112,000
 Low Range, 66% \$ 186,592,000

10.6 Other Data

Figures:

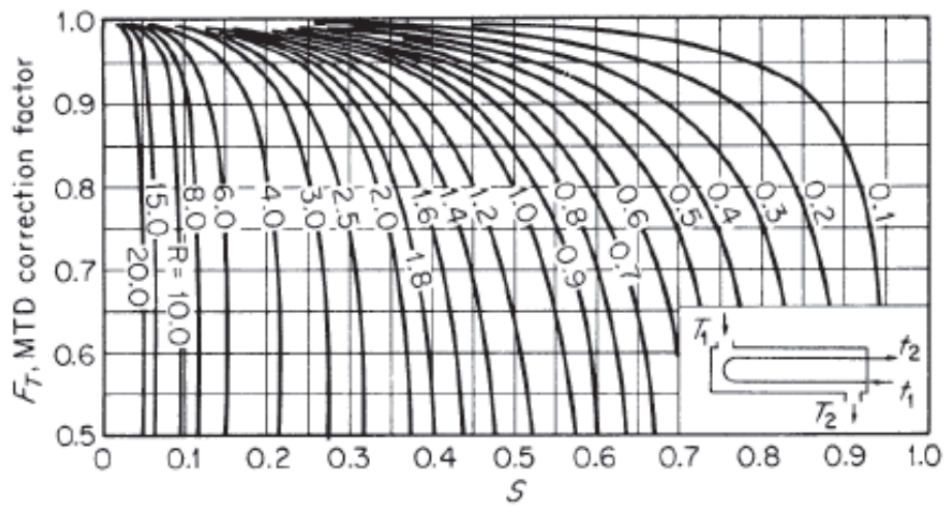


Figure 10-1: (Middleman, 1997) LMTD correction factor plot for a single shell and two tubes passes